cells were fixed with 4% paraformaldehyde in phosphate buffer for 15 min, attached to coverslips by cytospin, stained with FITC–anti-CD3ε, PE–anti-I-A/I-E, and anti-Sema4B–biotin plus streptavidin-Cy5, and then examined by confocal microscopy (Zeiss Exciter).

Western blot analysis

BM-derived basophils were starved for 16 h and then stimulated with IL-3 (30 ng/ml) in the presence of rSema4B- or hIgG-coated Dynabeads (Invitrogen). The cells were lysed at the indicated times with lysis buffer containing 1% Nonidet P40, 10 mM Tris-HCl, 150 mM NaCl, 1 mM EDTA, 10 mM Na_3Vo_4, 0.5 mM PMSF, 5 μg/ml leupeptin, 5 μg/ml aprotinin, 1 mM sodium orthovanadate, and a protease inhibitor mixture (Roche). Whole-cell lysates were separated by SDS-PAGE and then electrophoretically transferred to nitrocellulose membranes. The membranes were immunoblotted with various Abs.

Statistical analysis

Data are presented as mean ± SD. The p values were calculated with the two-tailed Student t test after the data were confirmed to fulfill the criteria. Otherwise, Mann–Whitney U test was performed.

Results

Sema4B is expressed in T and B cells

In a screen to identify semaphorins in the immune system, we isolated a cDNA fragment encoding a class IV semaphorin, Sema4B, through PCR-based cloning using degenerate oligonucleotide primers derived from motifs that are conserved across the semaphorin family. RT-PCR analyses showed that Sema4B was abundantly expressed in the spleen (Fig. 1*A*). Sema4B has been reported to play a role in assembling the postsynaptic specialization at glutamatergic and GABAergic synapses in the nervous system (34). However, the involvement of Sema4B in immune cell regulation has not been determined, and this led us to investigate the immunological function of Sema4B. To examine the expression of Sema4B in more detail, we generated an anti-Sema4B mAb that specifically recognizes Sema4B and does not cross-react with Sema4A or Sema4D (Fig. 1*B*). As shown in Fig. 1*C*, Sema4B is constitutively expressed in B and T cells, but not in DCs or basophils. To investigate the physiological role of Sema4B, we generated Sema4B$^{-/-}$ mice by deleting the fifth to eighth exons in the *Sema4B* gene (Fig. 1*D–F*). Sema4B$^{-/-}$ mice were born at the expected Mendelian ratio and were fertile. There were no apparent abnormalities based on gross macroscopic or histological examinations of all the tissues that express *Sema4B* transcripts.

Sema4B$^{-/-}$ mice have increased serum IgE levels

Immune cell populations, such as T cells, B cells, DCs, NK cells, and subpopulations of T cells, were normal in Sema4B$^{-/-}$ mice

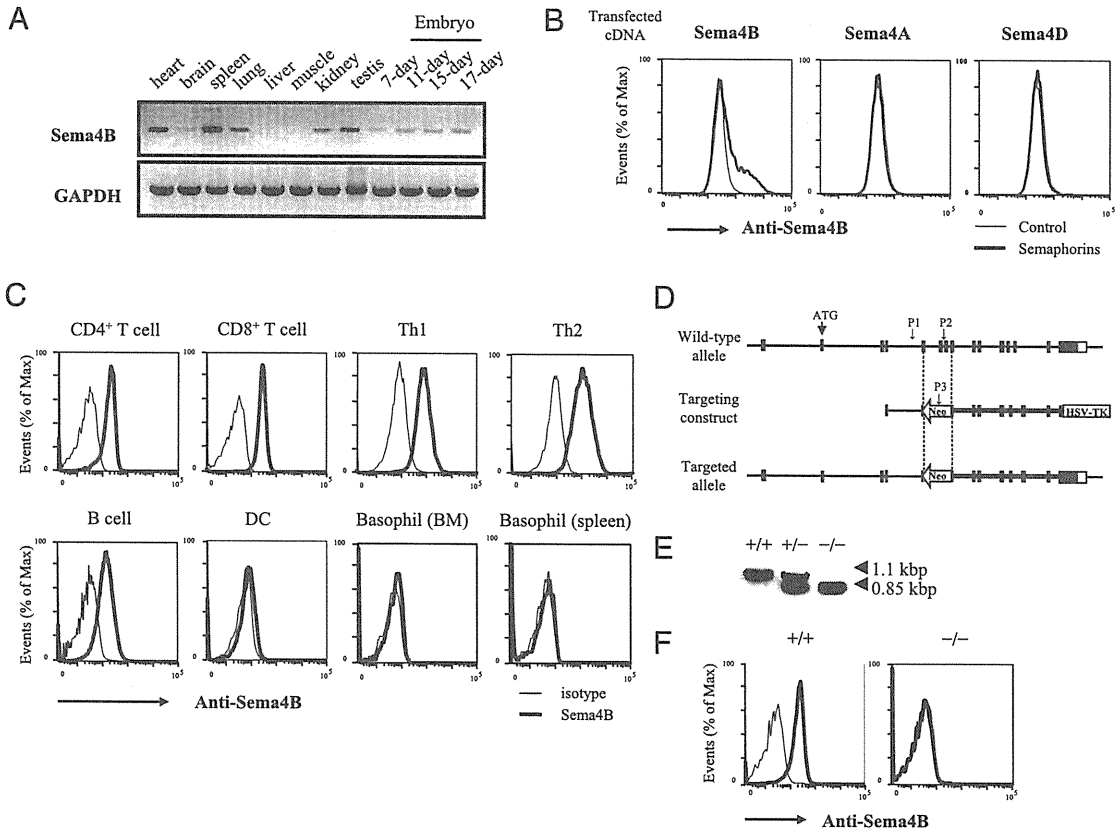

FIGURE 1. Sema4B is expressed in immune cells, especially T and B cells. *A*, Expression profiles of Sema4B. Sema4B transcripts were examined by RT-PCR using a panel of multiple mouse tissue cDNAs. GAPDH transcripts were used as controls. *B*, The anti-Sema4B Ab specifically binds to Sema4B. COS7 cells transfected with Sema4B, Sema4A, Sema4D expression constructs, or the control vector were stained with a biotinylated anti-Sema4B Ab (thick lines) or the isotype-matched control Ab (thin lines) followed by streptavidin-FITC. *C*, Sema4B is constitutively expressed in T and B cells. Mouse splenocytes, as well as BM-derived or fully differentiated Th1 or Th2 cells, were stained with anti-Sema4B (thick lines) or isotype-matched control (thin lines) Abs. *D*, Disruption of the *Sema4B* gene. The gene structures of the WT *Sema4B* allele (*top*), *Sema4B*-targeting construct (*middle*), and *Sema4B* mutant allele (*bottom*) are shown. Filled boxes denote the coding sequences. Exons 5 to 8 were replaced with a Neo cassette. The HSV thymidine kinase gene was added to select against random integration. *E*, Genomic typing analyses. Genomic DNA was isolated from the tails of WT (+/+), Sema4B heterozygous (+/−), and homozygous mutant mice (−/−), and the genotype was determined by PCR using the indicated primers. Arrowheads indicate the 1.1- and 0.85-kbp fragments that represent the WT allele and the targeted allele, respectively. *F*, Splenocytes from WT (+/+) and Sema4B$^{-/-}$ (−/−) mice were stained with FITC–anti-CD3 and biotinylated anti-Sema4B mAbs (thick lines) or isotype-matched controls (thin lines) plus streptavidin-allophycocyanin. The CD3$^+$ cells were gated and analyzed for Sema4B expression by flow cytometry.

Downloaded from www.jimmunol.org on June 14, 2011

(Supplemental Fig. 1). In vitro T cell-, B cell-, and DC-proliferative responses and cytokine production and T cell–DC interactions were not affected by the absence of Sema4B (Supplemental Fig. 2). However, Sema4B$^{-/-}$ mice had considerably increased serum IgE levels at steady-state, and these concentrations gradually increased as the mutant mice aged (Fig. 2*A*). We next examined T cell-dependent Ab responses in vivo, in which WT and Sema4B$^{-/-}$ mice were immunized with NP-CGG in alum and then boosted 2 wk after the first immunization. Interestingly, Sema4B$^{-/-}$ mice had considerably greater serum levels of IgE than WT mice, although the serum titers of NP-specific IgM, IgG1, and IgG2a were comparable between WT and Sema4B$^{-/-}$ mice (Fig. 2*B*). IgE production is tightly regulated by cell–cell interactions among T cells, B cells, and DCs (35). To explore the involvement of intrinsic Sema4B in IgE production by B cells, we examined Ab production from Sema4B$^{-/-}$ B cells. However, IgM, IgG1, and IgE production was comparable between WT and Sema4B$^{-/-}$ B cells (Fig. 2*C*) that were cultured with anti-CD40 and IL-4 in vitro. We then performed in vivo priming experiments by immunizing WT and Sema4B$^{-/-}$ mice in the hind footpads with KLH with CFA or alum. As shown in Fig. 2*D* and 2*E*, there were no differences in the generation of Ag-specific T cells in terms of proliferation and cytokine production between WT and Sema4B$^{-/-}$ mice. Furthermore, rSema4B had no effect on B cells, T cells, DCs, and T cell–DC interactions (Supplemental Fig. 3). These results strongly imply that non-B cell, non-T cell, and non-DC populations are responsible for the enhanced IgE production in Sema4B$^{-/-}$ mice.

Sema4B inhibits cytokine production from basophils

We then analyzed the basophil populations in the spleen and BM because basophil numbers have been shown to be critical for Th2 polarization and IgE production (5, 6). The proportion of basophils in WT and Sema4B$^{-/-}$ mice was comparable (Fig. 3*A*). We next examined whether rSema4B affects basophil responses. As shown in Fig. 3*B*, rSema4B bound to BM-derived basophils and significantly inhibited the ability of these cells to produce IL-4 and IL-6 in response to IL-3 stimulation (Fig. 3*C*), and these inhibitory effects were proportional to the rSema4B concentrations (Supplemental Fig. 4). It was previously reported that the FcRγ-mediated ITAM-spleen tyrosine kinase and its downstream mediator, ERK, are involved in IL-3–induced IL-4 production (30). In addition, IL-3Rβc–mediated JAK–STAT5 pathways are crucial for IL-3–induced proliferation (36, 37). As shown in Fig. 3*D*, ERK phosphorylation was inhibited by rSema4B, and similarly, STAT5 phosphorylation was inhibited by rSema4B (Fig. 3*E*). Basophils produce large amounts of IL-4 and IL-6 after being stimulated with cysteine proteases such as papain (9) or cross-linking of their surface IgE (12). rSema4B also inhibited IL-4 and IL-6 production from BM-derived basophils that were stimulated with papain or IgE anti-DNP and DNP-HSA (Fig. 3*F*, 3*G*). These results indicate that Sema4B negatively regulates cytokine production from basophils.

Sema4B suppresses basophil-mediated Th2 skewing

We examined whether rSema4B suppressed basophil-mediated Ag-specific Th2 skewing because basophils have been reported to promote Th2 polarization by functioning as APCs (38). To clarify this point, we cocultured OVA-TCR Tg-derived naive CD4$^+$ T cells with OVA peptide-pulsed BM-derived basophils for 5 d in the presence of rSema4B or hIgG. Interestingly, rSema4B significantly suppressed IL-4 but not IFN-γ production from T cells (Fig. 4*A*). Furthermore, when the basophil-T cell cocultures were

Downloaded from www.jimmunol.org on June 14, 2011

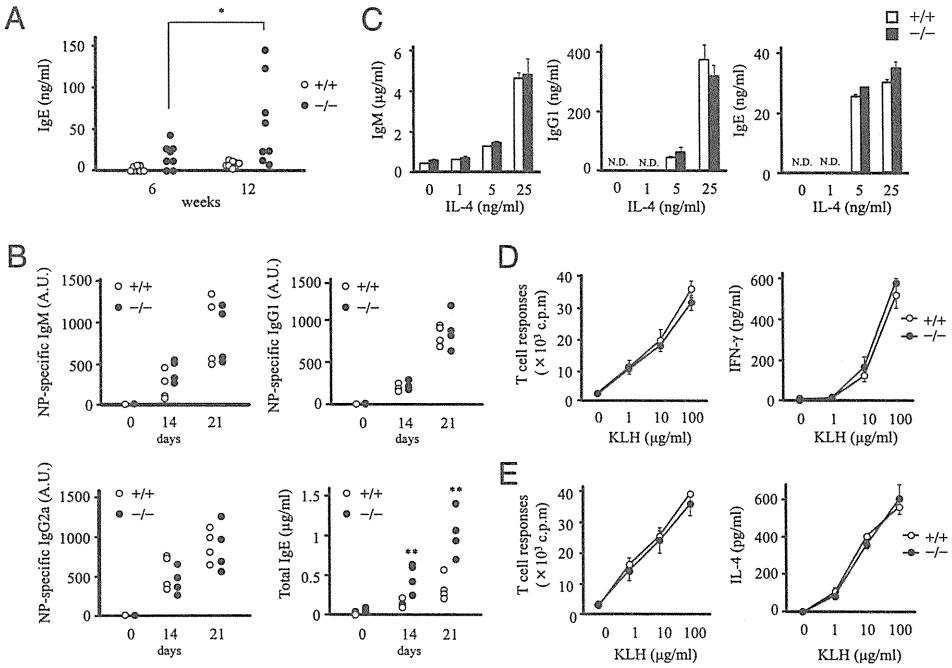

FIGURE 2. Sema4B$^{-/-}$ mice have increased serum IgE levels. *A*, Serum IgE levels in WT (open circles) and Sema4B$^{-/-}$ (closed circles) mice were measured at 6 and 12 wk by ELISA. *$p < 0.05$ (Mann–Whitney *U* test). *B*, WT (open circles) and Sema4B$^{-/-}$ (closed circles) mice were immunized i.p. with NP-CGG as an alum-precipitated complex on days 0 and 14, and bled at the indicated times. The anti-NP Ab titers were determined using NP-BSA–coated ELISA plates. The total IgE levels were determined by ELISA. **$p < 0.01$, ***$p < 0.005$ (Mann–Whitney *U* test). *C*, Purified splenic B cells from WT (open bars) or Sema4B$^{-/-}$ (closed bars) mice were stimulated with anti-CD40 and the indicated concentrations of IL-4. After 7 d, the IgM, IgG1, and IgE titers in the culture supernatants were measured by ELISA. *D* and *E*, WT (open circles) and Sema4B$^{-/-}$ (closed circles) mice were immunized in the hind footpads with KLH in CFA (*D*) or alum (*E*). Five days after priming, CD4$^+$ T cells prepared from the draining lymph nodes were restimulated with various concentrations of KLH and then examined for proliferation and cytokine production. Data are representative of two (*A*) or three (*B*–*E*) independent experiments.

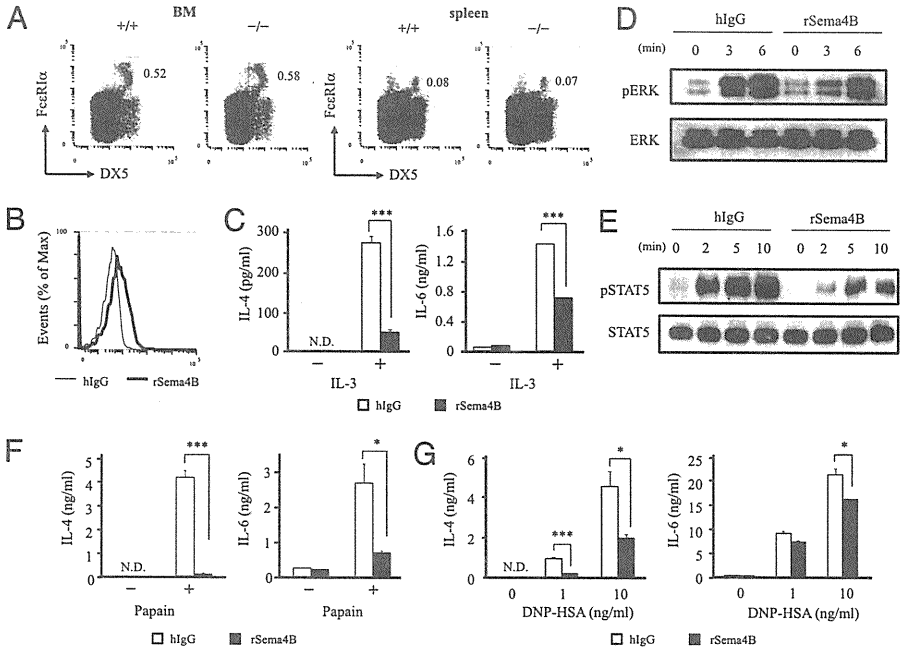

FIGURE 3. rSema4B inhibits cytokine production from basophils. *A*, Frequency of basophils in WT (+/+) and Sema4B$^{-/-}$ (−/−) mice. The numbers above the outlined areas indicate the percentages of FcεRIα^{+}DX5^{+} cells in the spleen or BM. *B*, BM-derived basophils were stained with biotinylated rSema4B (thick lines) or hIgG (thin lines) plus streptavidin-allophycocyanin. *C*, c-Kit–depleted and starved BM-derived basophils were stimulated with IL-3 in the presence of rSema4B (closed bars) or hIgG (open bars) for 16 h. The cytokine concentrations in the culture supernatants were measured by ELISA. *D* and *E*, c-Kit–depleted and starved BM-derived basophils were stimulated with IL-3 in the presence of rSema4B- or hIgG-coated beads. Cell lysates were prepared at the indicated times. The same amounts of protein extracts were immunoblotted using Abs against phospho-ERK and total ERK (*D*), or phospho-STAT5 and total STAT5 (*E*). *F* and *G*, c-Kit–depleted, BM-derived basophils were stimulated with papain (*F*) or IgE anti-DNP and various concentrations of DNP-HSA (*G*) for 16 h in the presence of rSema4B (closed bars) or hIgG (open bars). The cytokine concentrations in the culture supernatants were measured by ELISA. $*p < 0.05$, $***p < 0.005$ (Student *t* test). Data are representative of at least three independent experiments.

treated with papain and OVA or IgE cross-linking with IgE anti-DNP and DNP-OVA, Sema4B also significantly inhibited basophil-mediated Th2 skewing (Fig. 4*B*, 4*C*). Collectively, these findings suggest that Sema4B inhibits IL-4 production by basophils, resulting in suppression of basophil-mediated Th2 skewing.

Sema4B is highly expressed in CD4^{+} T cells (Fig. 1*C*). However, intrinsic Sema4B did not affect Th1 and Th2 differentiation in vitro (Supplemental Fig. 2*C*). To analyze whether T cell-derived Sema4B is critical for regulating basophil-mediated Th2 skewing, we cultured WT or Sema4B$^{-/-}$ OVA-TCR Tg-derived naive CD4^{+} T cells with BM-derived basophils and OVA peptide or DNP-OVA and IgE anti-DNP for 5 d. Sema4B$^{-/-}$ T cells showed considerably enhanced Th2 skewing (Fig. 4*D*, 4*E*). Next, to examine basophil-mediated Th2 skewing in vivo, we adoptively transferred WT or Sema4B$^{-/-}$ OVA-TCR Tg-derived naive CD4^{+} T cells into nude mice; then BM-derived basophils pulsed with DNP-OVA and IgE anti-DNP were intravenously transferred into these recipients. Four days later, we isolated CD4^{+} T cells from the spleen and examined the in vivo Th2 skewing of these CD4^{+} T cells. As shown in Fig. 4*F*, Sema4B$^{-/-}$ T cells had more T1/ST2^{+} Th2 cells and enhanced IL-4 production after being stimulated with DNP-OVA and BMDC (Fig. 4*G*). These results suggest that T cell-derived Sema4B is important for basophil-mediated Th2 skewing.

Basophils have been shown to form an immunological synapse with cognate T cells (11). The cytoplasmic tail of Sema4B contains a PDZ-binding motif and binds to postsynaptic density (PSD)-95 (39) that accumulates at contact sites between thymocytes and DCs (40). Thus, we next examined the localization of Sema4B during basophil and T cell interactions. Consistent with previous reports, papain-activated BM-derived basophils formed an immunological synapse with OVA-TCR Tg-derived CD4^{+} T cells in the presence of OVA peptide. Of note, Sema4B in T cells colocalized with CD3 and clustered at T cell–basophil contact sites (Fig. 4*H*). These results suggest that Sema4B in T cells accumulates at the immunological synapse and suppresses basophil functions in a cell–cell contact-dependent manner.

Sema4B$^{-/-}$ mice have enhanced IgE memory responses

During secondary Ag exposure, Ag-specific, IgE-bearing basophils capture Ag, become activated, and secrete cytokines, which subsequently facilitates memory B cell responses (7, 41). Although WT and Sema4B$^{-/-}$ basophils produced comparable levels of IL-4 and IL-6 on FcεRI cross-linking (Supplemental Fig. 5), the serum IgE concentrations increased with age in Sema4B$^{-/-}$ mice (Fig. 2*A*). We hypothesized that this phenomenon can be caused not only by basophil-mediated priming responses but by basophil-mediated memory responses. To determine whether Sema4B is involved in immunological memory responses, we immunized WT and Sema4B$^{-/-}$ mice with OVA proteins and then boosted them with OVA proteins. Sema4B$^{-/-}$ mice had significantly greater levels of serum OVA-specific IgG1 and IgE than WT mice (Fig. 5*A*). Furthermore, the increased IgG1 and IgE responses in Sema4B$^{-/-}$ mice were suppressed when basophils were depleted before the secondary immunization (Fig. 5*B*), which suggests that basophils are responsible for the enhanced memory responses in Sema4B$^{-/-}$ mice. Taken together, these results indicate that Sema4B also negatively regulates basophil-mediated humoral memory responses.

Discussion

Semaphorins have been shown to play crucial roles in the immune system (21). In this study, we performed a screen to identify novel

Downloaded from www.jimmunol.org on June 14, 2011

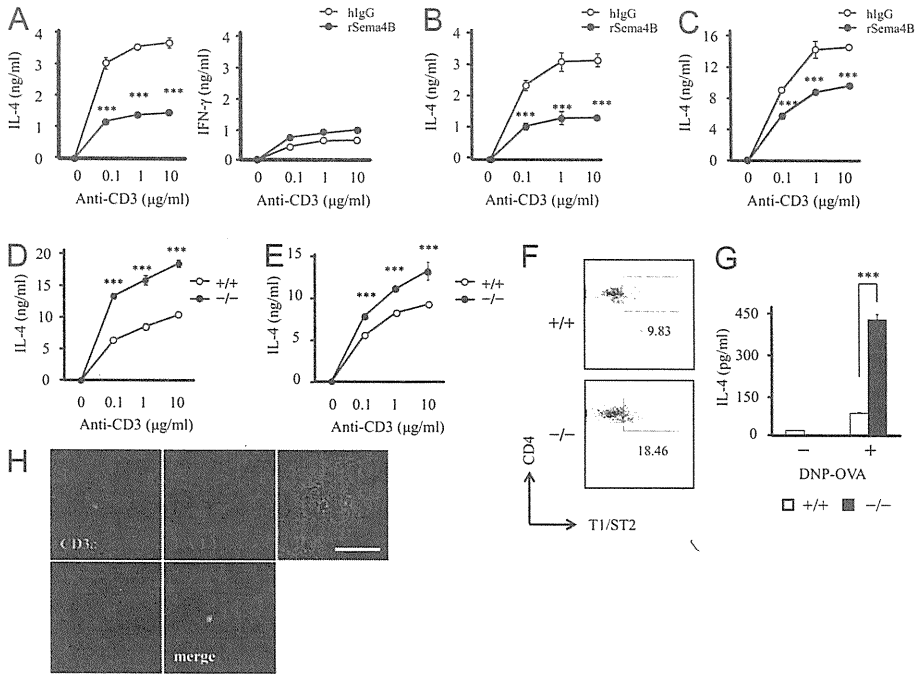

FIGURE 4. Sema4B negatively regulates basophil-mediated Th2 skewing. *A–C*, OVA-TCR Tg-derived naive $CD4^+CD62L^+$ T cells and irradiated BM-derived basophils ($CD11c^-$c-$Kit^-Fc\varepsilon RI\alpha^+$) were cultured with OVA peptide (*A*), papain and OVA (*B*), or IgE anti-DNP and DNP-OVA (*C*) in the presence of rSema4B (closed circles) or hIgG (open circles) for 5 d. Then the $CD4^+$ T cells isolated by anti-CD4–conjugated magnetic beads were restimulated with various concentrations of immobilized anti-CD3 for 24 h. The cytokine concentrations in the culture supernatants were measured by ELISA. *D* and *E*, WT (open circles) or $Sema4B^{-/-}$ (closed circles) OVA-TCR Tg-derived naive $CD4^+CD62L^+$ T cells and irradiated BM-derived basophils ($CD11c^-$c-Kit^- $Fc\varepsilon RI\alpha^+$) were cultured with OVA peptide (*D*) or IgE anti-DNP and DNP-OVA (*E*) for 5 d. Then the $CD4^+$ T cells isolated by anti-CD4–conjugated magnetic beads were restimulated with various concentrations of immobilized anti-CD3 for 24 h. The cytokine concentrations in the culture supernatants were measured by ELISA. *F* and *G*, WT (+/+ or open bars) or $Sema4B^{-/-}$ (−/− or closed bars) OVA-TCR Tg-derived naive $CD4^+CD62L^+$ T cells were i.v. transferred into nude mice. The next day, BM-derived basophils ($CD11c^-$c-$Kit^-Fc\varepsilon RI\alpha^+$) pulsed with IgE anti-DNP and DNP-OVA were i.v. transferred into these recipients. Four days later, $CD4^+$ T cells isolated from these mice were stained with anti-CD4 and anti-T1/ST2 (*F*), and cultured with BMDC and DNP-OVA for 36 h (*G*). The cytokine concentrations in the culture supernatants were measured by ELISA. $^{***}p < 0.005$ (Student *t* test). *H*, Papain-activated, BM-derived basophils ($CD11c^-$c-Kit^-DX5^+) and OVA TCR Tg-derived $CD4^+$ T cells were cocultured with OVA peptide for 1 h and then fixed in 4% paraformaldehyde phosphate buffer. Then the cells were attached to coverslips by cytospin and stained with FITC–anti-CD3ε (green), PE–anti-I-A/I-E (red) and anti-Sema4B–biotin plus streptavidin-Cy5 (blue). The localization of Sema4B was evaluated by confocal microscopy. Scale bar, 10 μm.

immune semaphorins that function in the immune system and determined that Sema4B, which is abundantly expressed in lymphocytes, suppresses the functions of basophils and regulates both the homeostatic Th1/Th2 balance and immunological memory responses. Our findings identified not only a novel immune semaphorin but also an important regulatory mechanism for basophils.

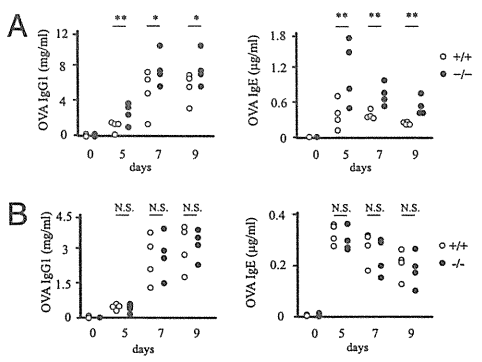

FIGURE 5. $Sema4B^{-/-}$ mice exhibit enhanced humoral memory responses. *A*, WT (open circles) and $Sema4B^{-/-}$ (closed circles) mice were immunized i.p. with OVA without adjuvant and then rechallenged i.v. with OVA after 4 wk. OVA-specific IgG1 and IgE in the serum were measured at the indicated times by ELISA. *B*, WT (open circles) and $Sema4B^{-/-}$ (closed circles) mice were primarily immunized as described earlier and then depleted of basophils. Two days after the final injection of anti-FcεRIα, the mice were rechallenged with OVA. The OVA-specific IgG1 and IgE levels were measured by ELISA. $^*p < 0.05$, $^{**}p < 0.01$ (Mann–Whitney *U* test).

In this article, we show that Sema4B significantly inhibited IL-4 and IL-6 production by basophils in response to various stimuli, including IL-3, papain, and FcεRI cross-linking. Because of the fact that Sema4B regulates cytokine production, basophil-mediated Th2 skewing was also inhibited. In addition, we showed that a Sema4B deficiency in T cells results in increased Th2 responses, suggesting that Sema4B negatively regulates basophils. Basophils are shown to facilitate Th2 skewing and IgE production, and serve as a cellular source for IL-4 and IL-6 (4). In addition, recent reports have shown that Ag-capturing basophils can function as APCs and induce Th2 responses in an IL-4–dependent manner (12). In contrast, several reports have claimed that basophils only minimally function as APCs during in vivo inflammatory conditions such as helminthic infections (15) and allergic responses induced by the house dust mite allergen (13), in which DCs played vital roles in Th2 development. In addition, $CD11c^+Fc\varepsilon RI\alpha^+$ DCs have been detected in IL-3–conditioned BM cultures (13), which raise a possibility that a subpopulation of DCs remained in the basophil fraction. To exclude this possibility, we prepared BM-derived basophils by sorting for the $CD11c^-$ c-$Kit^-Fc\varepsilon RI\alpha^+$ fraction. However, these cells still induced naive $CD4^+$ T cells to become Th2 cells. In addition, rSema4B did not affect DCs in terms of cytokine production and cognate T cell

Downloaded from www.jimmunol.org on June 14, 2011

activation. Although we cannot completely exclude a possible involvement of endogenous DCs, our findings indicate that the effects of T cell-derived Sema4B on basophils would be primarily responsible for in vivo Th2 skewing in our adoptive transfer experiments. In addition, we found that Sema4B expression on T cells was upregulated by anti-CD3 stimulation (data not shown), and that Sema4B localized at the contact sites between basophils and $CD4^+$ T cells. It was reported that the PDZ-binding motif in the C terminus of Sema4B binds to PSD-95 (39), and that PSD-95 in T cells preferentially localizes at contact sites during cell–cell interactions (40). In this context, our data strongly imply that basophils are regulated through cell–cell contact, in which Sema4B negatively regulates basophil functions.

It has been thought that basophils are predominant Ag-capturing cells (41), and that Ag and Ag-specific IgE complexes activate basophils to produce IL-4 and IL-6, leading to enhanced humoral memory immune responses (7). However, a recent report showed that basophil-deficient mice still have efficient humoral immune responses (14). It has been reported that DCs have a considerably greater potential to function as APCs than basophils (13, 15, 16), suggesting that DCs overcome basophil functions depending on the experimental conditions, including the Ag dose and the use of adjuvants. However, $Sema4B^{-/-}$ mice that were immunized with Ag without adjuvant and administered small amounts of Ag i.v. displayed enhanced Ag-specific IgE production. In addition, depleting basophils with an anti-FcεRIα Ab abolished the enhanced IgE production in $Sema4B^{-/-}$ mice. It thus appears that the impaired negative regulation on basophils is responsible for enhanced humoral memory responses in $Sema4B^{-/-}$ mice.

Sema4B not only suppressed FcεRI cross-linking–induced cytokine production by basophils (Fig. 3*G*) but negatively regulated Th2 skewing in a cell–cell contact-dependent manner (Fig. 4*D*, 4*E*). Therefore, it is plausible that enhanced humoral memory responses in Sema4B-deficient mice are due to soluble cytokines, as well as cell–cell contact-dependent mechanisms, although further studies would be required to determine the definitive Sema4B mode. Of note, recent reports have shown that more basophils enhanced steady-state Th2 polarization and increased serum IgE levels (5, 6), suggesting that basophils control the homeostatic Th1/Th2 balance even in the steady-state conditions. In this context, it appears that the defects in the regulatory effects of Sema4B on basophils during both priming and memory phases can contribute to the increased serum IgE levels in $Sema4B^{-/-}$ mice as they aged.

Regarding the signaling mechanism for Sema4B-mediated basophil functions, we showed that Sema4B suppressed the IL-3–induced phosphorylation of ERK and STAT5, suggesting that Sema4B regulates IL-3 signaling. IL-3–mediated signals in basophils are reportedly involved in the ITAM in the FcRγ-spleen tyrosine kinase-ERK pathway to produce IL-4 and the IL-3Rβc–JAK-STAT5 pathway to promote proliferation and differentiation (30, 36, 37). Recently, it was shown that SHIP inhibited IL-4 production from basophils (42). In addition, *Src* homology 2 domain-containing protein tyrosine-phosphatase 1 (SHP-1) can interact with and inhibit the phosphorylation of STAT5 (43, 44). These inhibitory molecules are phosphatases that are mainly recruited to ITIM-containing receptors (45). Although it remains unclear whether ITIM-containing receptor is directly involved in IL-3–mediated signals in basophils, it is possible that Sema4B may regulate basophil functions through ITIM-containing molecules. Regarding the receptors for class IV semaphorins, several molecules such as plexin-Bs (B1, B2, B3) (46), plexin-D1 (47), T cell Ig and mucin domain-containing molecule-2 (Tim2) (24), and CD72 (23) have been shown to bind to class IV semaphorins. In fact, many of these molecules are expressed by basophils as determined by RT-PCR (data not shown). Additional investigations, including the identification of the Sema4B receptor, are required to further examine these mechanisms.

In conclusion, we demonstrated that Sema4B suppressed IL-4 production from basophils, in which T cell-derived Sema4B inhibited basophil-mediated Th2 skewing. In addition, a Sema4B deficiency significantly affected Ag-specific IgE memory responses, possibly in a cell–cell contact-dependent manner. Thus, Sema4B negatively regulates basophil functions during both primary and memory responses. These findings not only provide new insight into mechanisms that regulate basophils but identify a novel therapeutic target for allergic diseases.

Acknowledgments

We thank T. Yazawa for technical support.

Disclosures

The authors have no financial conflicts of interest.

References

1. Kawakami, T., and S. J. Galli. 2002. Regulation of mast-cell and basophil function and survival by IgE. *Nat. Rev. Immunol.* 2: 773–786.
2. Anthony, R. M., L. I. Rutitzky, J. F. Urban, Jr., M. J. Stadecker, and W. C. Gause. 2007. Protective immune mechanisms in helminth infection. *Nat. Rev. Immunol.* 7: 975–987.
3. Min, B. 2008. Basophils: what they 'can do' versus what they 'actually do'. *Nat. Immunol.* 9: 1333–1339.
4. Sullivan, B. M., and R. M. Locksley. 2009. Basophils: a nonredundant contributor to host immunity. *Immunity* 30: 12–20.
5. Hida, S., M. Tadachi, T. Saito, and S. Taki. 2005. Negative control of basophil expansion by IRF-2 critical for the regulation of Th1/Th2 balance. *Blood* 106: 2011–2017.
6. Charles, N., W. T. Watford, H. L. Ramos, L. Hellman, H. C. Oettgen, G. Gomez, J. J. Ryan, J. J. O'Shea, and J. Rivera. 2009. Lyn kinase controls basophil GATA-3 transcription factor expression and induction of Th2 cell differentiation. *Immunity* 30: 533–543.
7. Denzel, A., U. A. Maus, M. Rodriguez Gomez, C. Moll, M. Niedermeier, C. Winter, R. Maus, S. Hollingshead, D. E. Briles, L. A. Kunz-Schughart, et al. 2008. Basophils enhance immunological memory responses. *Nat. Immunol.* 9: 733–742.
8. Seder, R. A., W. E. Paul, A. M. Dvorak, S. J. Sharkis, A. Kagey-Sobotka, Y. Niv, F. D. Finkelman, S. A. Barbieri, S. J. Galli, and M. Plaut. 1991. Mouse splenic and bone marrow cell populations that express high-affinity Fc epsilon receptors and produce interleukin 4 are highly enriched in basophils. *Proc. Natl. Acad. Sci. USA* 88: 2835–2839.
9. Sokol, C. L., G. M. Barton, A. G. Farr, and R. Medzhitov. 2008. A mechanism for the initiation of allergen-induced T helper type 2 responses. *Nat. Immunol.* 9: 310–318.
10. Perrigoue, J. G., S. A. Saenz, M. C. Siracusa, E. J. Allenspach, B. C. Taylor, P. R. Giacomin, M. G. Nair, Y. Du, C. Zaph, N. van Rooijen, et al. 2009. MHC class II-dependent basophil-CD4+ T cell interactions promote T(H)2 cytokine-dependent immunity. *Nat. Immunol.* 10: 697–705.
11. Sokol, C. L., N. Q. Chu, S. Yu, S. A. Nish, T. M. Laufer, and R. Medzhitov. 2009. Basophils function as antigen-presenting cells for an allergen-induced T helper type 2 response. *Nat. Immunol.* 10: 713–720.
12. Yoshimoto, T., K. Yasuda, H. Tanaka, M. Nakahira, Y. Imai, Y. Fujimori, and K. Nakanishi. 2009. Basophils contribute to T(H)2-IgE responses in vivo via IL-4 production and presentation of peptide-MHC class II complexes to CD4+ T cells. *Nat. Immunol.* 10: 706–712.
13. Hammad, H., M. Plantinga, K. Deswarte, P. Pouliot, M. A. Willart, M. Kool, F. Muskens, and B. N. Lambrecht. 2010. Inflammatory dendritic cells—not basophils—are necessary and sufficient for induction of Th2 immunity to inhaled house dust mite allergen. *J. Exp. Med.* 207: 2097–2111.
14. Ohnmacht, C., C. Schwartz, M. Panzer, I. Schiedewitz, R. Naumann, and D. Voehringer. 2010. Basophils orchestrate chronic allergic dermatitis and protective immunity against helminths. *Immunity* 33: 364–374.
15. Phythian-Adams, A. T., P. C. Cook, R. J. Lundie, L. H. Jones, K. A. Smith, T. A. Barr, K. Hochweller, S. M. Anderton, G. J. Hämmerling, R. M. Maizels, and A. S. MacDonald. 2010. CD11c depletion severely disrupts Th2 induction and development in vivo. *J. Exp. Med.* 207: 2089–2096.
16. Tang, H., W. Cao, S. P. Kasturi, R. Ravindran, H. I. Nakaya, K. Kundu, N. Murthy, T. B. Kepler, B. Malissen, and B. Pulendran. 2010. The T helper type 2 response to cysteine proteases requires dendritic cell-basophil cooperation via ROS-mediated signaling. *Nat. Immunol.* 11: 608–617.
17. Kolodkin, A. L., D. J. Matthes, and C. S. Goodman. 1993. The semaphorin genes encode a family of transmembrane and secreted growth cone guidance molecules. *Cell* 75: 1389–1399.
18. Serini, G., D. Valdembri, S. Zanivan, G. Morterra, C. Burkhardt, F. Caccavari, L. Zammataro, L. Primo, L. Tamagnone, M. Logan, et al. 2003. Class 3

Downloaded from www.jimmunol.org on June 14, 2011

semaphorins control vascular morphogenesis by inhibiting integrin function. *Nature* 424: 391–397.
19. Toyofuku, T., H. Zhang, A. Kumanogoh, N. Takegahara, F. Suto, J. Kamei, K. Aoki, M. Yabuki, M. Hori, H. Fujisawa, and H. Kikutani. 2004. Dual roles of Sema6D in cardiac morphogenesis through region-specific association of its receptor, Plexin-A1, with off-track and vascular endothelial growth factor receptor type 2. *Genes Dev.* 18: 435–447.
20. Neufeld, G., and O. Kessler. 2008. The semaphorins: versatile regulators of tumour progression and tumour angiogenesis. *Nat. Rev. Cancer* 8: 632–645.
21. Suzuki, K., A. Kumanogoh, and H. Kikutani. 2008. Semaphorins and their receptors in immune cell interactions. *Nat. Immunol.* 9: 17–23.
22. Capparuccia, L., and L. Tamagnone. 2009. Semaphorin signaling in cancer cells and in cells of the tumor microenvironment—two sides of a coin. *J. Cell Sci.* 122: 1723–1736.
23. Kumanogoh, A., C. Watanabe, I. Lee, X. Wang, W. Shi, H. Araki, H. Hirata, K. Iwahori, J. Uchida, T. Yasui, et al. 2000. Identification of CD72 as a lymphocyte receptor for the class IV semaphorin CD100: a novel mechanism for regulating B cell signaling. *Immunity* 13: 621–631.
24. Kumanogoh, A., S. Marukawa, K. Suzuki, N. Takegahara, C. Watanabe, E. Ch'ng, I. Ishida, H. Fujimura, S. Sakoda, K. Yoshida, and H. Kikutani. 2002. Class IV semaphorin Sema4A enhances T-cell activation and interacts with Tim-2. *Nature* 419: 629–633.
25. Takegahara, N., H. Takamatsu, T. Toyofuku, T. Tsujimura, T. Okuno, K. Yukawa, M. Mizui, M. Yamamoto, D. V. Prasad, K. Suzuki, et al. 2006. Plexin-A1 and its interaction with DAP12 in immune responses and bone homeostasis. *Nat. Cell Biol.* 8: 615–622.
26. Kumanogoh, A., T. Shikina, K. Suzuki, S. Uematsu, K. Yukawa, S. Kashiwamura, H. Tsutsui, M. Yamamoto, H. Takamatsu, E. P. Ko-Mitamura, et al. 2005. Nonredundant roles of Sema4A in the immune system: defective T cell priming and Th1/Th2 regulation in Sema4A-deficient mice. *Immunity* 22: 305–316.
27. Takamatsu, H., N. Takegahara, Y. Nakagawa, M. Tomura, M. Taniguchi, R. H. Friedel, H. Rayburn, M. Tessier-Lavigne, Y. Yoshida, T. Okuno, et al. 2010. Semaphorins guide the entry of dendritic cells into the lymphatics by activating myosin II. *Nat. Immunol.* 11: 594–600.
28. Sato, T., T. Sasahara, Y. Nakamura, T. Osaki, T. Hasegawa, T. Tadakuma, Y. Arata, Y. Kumagai, M. Katsuki, and S. Habu. 1994. Naive T cells can mediate delayed-type hypersensitivity response in T cell receptor transgenic mice. *Eur. J. Immunol.* 24: 1512–1516.
29. Yoshimoto, T., H. Tsutsui, K. Tominaga, K. Hoshino, H. Okamura, S. Akira, W. E. Paul, and K. Nakanishi. 1999. IL-18, although antiallergic when administered with IL-12, stimulates IL-4 and histamine release by basophils. *Proc. Natl. Acad. Sci. USA* 96: 13962–13966.
30. Hida, S., S. Yamasaki, Y. Sakamoto, M. Takamoto, K. Obata, T. Takai, H. Karasuyama, K. Sugane, T. Saito, and S. Taki. 2009. Fc receptor gamma-chain, a constitutive component of the IL-3 receptor, is required for IL-3-induced IL-4 production in basophils. *Nat. Immunol.* 10: 214–222.
31. Inaba, K., R. M. Steinman, M. W. Pack, H. Aya, M. Inaba, T. Sudo, S. Wolpe, and G. Schuler. 1992. Identification of proliferating dendritic cell precursors in mouse blood. *J. Exp. Med.* 175: 1157–1167.
32. Doi, T., K. Obayashi, T. Kadowaki, H. Fujii, and S. Koyasu. 2008. PI3K is a negative regulator of IgE production. *Int. Immunol.* 20: 499–508.
33. Shi, W., A. Kumanogoh, C. Watanabe, J. Uchida, X. Wang, T. Yasui, K. Yukawa, M. Ikawa, M. Okabe, J. R. Parnes, et al. 2000. The class IV semaphorin CD100 plays nonredundant roles in the immune system: defective B and T cell activation in CD100-deficient mice. *Immunity* 13: 633–642.
34. Paradis, S., D. B. Harrar, Y. Lin, A. C. Koon, J. L. Hauser, E. C. Griffith, L. Zhu, L. F. Brass, C. Chen, and M. E. Greenberg. 2007. An RNAi-based approach identifies molecules required for glutamatergic and GABAergic synapse development. *Neuron* 53: 217–232.
35. Geha, R. S., H. H. Jabara, and S. R. Brodeur. 2003. The regulation of immunoglobulin E class-switch recombination. *Nat. Rev. Immunol.* 3: 721–732.
36. Reddy, E. P., A. Korapati, P. Chaturvedi, and S. Rane. 2000. IL-3 signaling and the role of Src kinases, JAKs and STATs: a covert liaison unveiled. *Oncogene* 19: 2532–2547.
37. Martinez-Moczygemba, M., and D. P. Huston. 2003. Biology of common beta receptor-signaling cytokines: IL-3, IL-5, and GM-CSF. *J. Allergy Clin. Immunol.* 112: 653–665, quiz 666.
38. Sokol, C. L., and R. Medzhitov. 2010. Emerging functions of basophils in protective and allergic immune responses. *Mucosal Immunol.* 3: 129–137.
39. Burkhardt, C., M. Müller, A. Badde, C. C. Garner, E. D. Gundelfinger, and A. W. Püschel. 2005. Semaphorin 4B interacts with the post-synaptic density protein PSD-95/SAP90 and is recruited to synapses through a C-terminal PDZ-binding motif. *FEBS Lett.* 579: 3821–3828.
40. Affaticati, P., O. Mignen, F. Jambou, M. C. Potier, I. Klingel-Schmitt, J. Degrouard, S. Peineau, E. Gouadon, G. L. Collingridge, R. Liblau, et al. 2011. Sustained calcium signalling and caspase-3 activation involve NMDA receptors in thymocytes in contact with dendritic cells. *Cell Death Differ.* 18: 99–108.
41. Mack, M., M. A. Schneider, C. Moll, J. Cihak, H. Brühl, J. W. Ellwart, M. P. Hogarth, M. Stangassinger, and D. Schlöndorff. 2005. Identification of antigen-capturing cells as basophils. *J. Immunol.* 174: 735–741.
42. Kuroda, E., V. Ho, J. Ruschmann, F. Antignano, M. Hamilton, M. J. Rauh, A. Antov, R. A. Flavell, L. M. Sly, and G. Krystal. 2009. SHIP represses the generation of IL-3-induced M2 macrophages by inhibiting IL-4 production from basophils. *J. Immunol.* 183: 3652–3660.
43. Paling, N. R., and M. J. Welham. 2002. Role of the protein tyrosine phosphatase SHP-1 (Src homology phosphatase-1) in the regulation of interleukin-3-induced survival, proliferation and signalling. *Biochem. J.* 368: 885–894.
44. Minoo, P., M. M. Zadeh, R. Rottapel, J. J. Lebrun, and S. Ali. 2004. A novel SHP-1/Grb2-dependent mechanism of negative regulation of cytokine-receptor signaling: contribution of SHP-1 C-terminal tyrosines in cytokine signaling. *Blood* 103: 1398–1407.
45. Kraft, S., and J. P. Kinet. 2007. New developments in FcepsilonRI regulation, function and inhibition. *Nat. Rev. Immunol.* 7: 365–378.
46. Pasterkamp, R. J., and A. L. Kolodkin. 2003. Semaphorin junction: making tracks toward neural connectivity. *Curr. Opin. Neurobiol.* 13: 79–89.
47. Toyofuku, T., M. Yabuki, J. Kamei, M. Kamei, N. Makino, A. Kumanogoh, and M. Hori. 2007. Semaphorin-4A, an activator for T-cell-mediated immunity, suppresses angiogenesis via Plexin-D1. *EMBO J.* 26: 1373–1384.

Downloaded from www.jimmunol.org on June 14, 2011

 DOI 10.1002/eji.201040930 Eur. J. Immunol. 2011. 41: 1420–1434

European Journal of Immunology

Steady state migratory RelB$^+$ langerin$^+$ dermal dendritic cells mediate peripheral induction of antigen-specific CD4$^+$CD25$^+$Foxp3$^+$ regulatory T cells

Hiroaki Azukizawa[*1,2], *Anja Döhler*[*3], *Nobuo Kanazawa*[1], *Arnab Nayak*[4], *Martin Lipp*[5], *Bernard Malissen*[6], *Ingo Autenrieth*[7], *Ichiro Katayama*[2], *Marc Riemann*[8], *Falk Weih*[8], *Friederike Berberich-Siebelt*[4] *and Manfred B. Lutz*[1,3]

[1] Department of Dermatology, University Hospital Erlangen, Erlangen, Germany
[2] Course of Integrated Medicine, Osaka University, Graduate School of Medicine, Suita, Japan
[3] Institute of Virology and Immunobiology, University of Würzburg, Würzburg, Germany
[4] Institute of Pathology, University of Würzburg, Würzburg, Germany
[5] Max-Delbrück-Center for Molecular Medicine, Berlin, Germany
[6] Centre d'Immunologie de Marseille-Luminy, INSERM U631, CNRS UMR6102 Université de la Méditerrannée, Marseille France
[7] Institute for Medical Microbiology, University of Tübingen, Germany
[8] Leibniz-Institute for Age Research – Fritz-Lipmann-Institute, Jena, Germany

Tolerance to self-antigens expressed in peripheral organs is maintained by CD4$^+$ CD25$^+$ Foxp3$^+$ Treg cells, which are generated as a result of thymic selection or peripheral induction. Here, we demonstrate that steady-state migratory DCs from the skin mediated Treg conversion in draining lymph nodes of mice. These DCs displayed a partially mature MHC II^{int} CD86^{int} CD40^{hi} CCR7$^+$ phenotype, used endogenous TGF-β for conversion and showed nuclear RelB translocation. Deficiency of the alternative NF-κB signaling pathway (RelB/p52) reduced steady-state migration of DCs. These DCs transported and directly presented soluble OVA provided by s.c. implanted osmotic minipumps, as well as cell-associated epidermal OVA in transgenic K5-mOVA mice to CD4$^+$ OVA-specific TCR-transgenic OT-II T cells. The langerin$^+$ dermal DC subset, but not epidermal Langerhans cells, mediated conversion of naive OT-II × RAG-1$^{-/-}$ T cells into proliferating CD4$^+$ CD25$^+$ Foxp3$^+$ Tregs. Thus, our data suggest that steady-state migratory RelB$^+$ TGF-β$^+$ langerin$^+$ dermal DCs mediate peripheral Treg conversion in response to epidermal antigen in skin-draining lymph nodes.

Keywords: Cell trafficking · DCs · Immune regulation · Tolerance · Treg cells


Supporting Information available online

Introduction

Immature DCs reside in peripheral tissues where they capture antigens of various types. Recognition of pathogenic structures then initiates DC maturation and migration to draining lymph nodes for induction of immunity against the transported pathogens [1]. Also, under steady-state conditions immature DCs capture and present antigens in secondary lymphoid organs, presumably to induce tolerance [2, 3]. These immature DCs are attached to the lymph node reticular conduit system where small

Correspondence: Dr. Manfred B. Lutz
e-mail: m.lutz@vim.uni-wuerzburg.de

*These authors contributed equally to this work.

© 2011 WILEY-VCH Verlag GmbH & Co. KGaA, Weinheim

antigens drained from peripheral tissues can be taken up from the fluid phase for presentation to T cells under steady-state conditions [4]. Recently, it has been reported that continuous peripheral antigen delivery can induce Treg conversion in draining lymph nodes. This suggests that the reticular conduit system delivers exogenous peptides under non-immunogenic conditions, which can be mimicked by implanted osmotic pumps, to lymph node-resident immature DCs, which then present these peptides to induce Tregs in vivo [5].

Such mechanisms of antigen delivery may explain the induction of $CD4^+$ T-cell anergy as shown for antigen presentation by immature DCs expressing only low levels of MHC II and costimulatory molecules [6]. However, it does not explain how immature DCs may induce $CD4^+$ Treg since B7-1/B7-$2^{-/-}$ and $CD28^{-/-}$ mice lack $CD4^+$ $CD25^+$ Tregs despite the presence of immature DCs [7]. Splenic DCs converted Treg better than B cells, and CD80/86-deficiency of the DCs further increases the conversion. These conversion experiments were either in vitro studies or under a pathological situation (tumor) but not steady state [8]. Later, the splenic $CD8\alpha^+$ DC subset was identified as mediating conversion after injection of a DEC205-targeting antibody [9]. The physiological relevance of splenic DCs or DEC205 for Treg conversion with self-antigens remains open. A $CD103^+$ DC population has been isolated from mesenteric lymph nodes that mediated TGF-β-dependent Treg conversion in culture, but the maturation stage of the DC has not been analyzed [10]. In contrast, a $CD103^-$ DC subset within skin-draining lymph nodes was responsible for Treg conversion in vitro [11]. This indicates that CD103 expression by DCs is not correlated with their capacity to convert Tregs and a specific phenotype for DCs inducing Tregs under steady-state conditions and in vivo remains to be identified [12].

Fluid phase soluble antigen transport also does not explain how lymph node T cells can be tolerized against cell-associated antigens. Therefore, the presentation of self-antigens by migratory DCs has been suggested as a mechanism of peripheral tolerance since these cells can be observed in draining lymph nodes of various organs [13, 14]. The mature CCR7-expressing DC fraction within peripheral skin-draining lymph nodes of mice has been identified as consisting of migrated Langerhans cells (LCs) and dermal DCs [14, 15].

We have shown previously that in vitro generated and TNF-matured DCs differentiated into a semi-mature phenotype could tolerogenic [16] and, in other systems such as inflammation-mediated DC maturation, were unable to differentiate immunogenic $CD4^+$ T helper cells [17]. Therefore, semi-mature DCs with tolerogenic potential can be distinguished from fully matured DCs with immunogenic functions [13]. The demonstration of the presence and function of such a partially mature and tolerogenic DC phenotype in vivo, however, remained open.

Three subsets of migratory DCs have been identified in skin-draining lymph nodes of mice, which consist of epidermal $langerin^+$ LCs and two subsets of $langerin^+$ and $langerin^-$ dermal DCs [18–20]. Recent evidence suggests that in the K5-mOVA mouse model cross-tolerance of OVA-specific $CD8^+$ OT-I T cells to this epidermal neo-self-antigen is mediated predominantly by the $CD103^+$ $langerin^+$ dermal DCs but not the other subtypes [21, 22].

Here, we found no clear correlation for CD103 as a marker for steady-state migratory DCs but that extrathymic self-antigen presentation by skin-derived $RelB^+$ $langerin^+$ dermal DCs results in the de novo generation of $Foxp3^+$ Tregs in the periphery.

Results

Skin-draining lymph nodes contain resident immature and migratory semi-mature DCs in the steady state

As reported by others before [14, 23] skin-draining lymph nodes of WT but not $CCR7^{-/-}$ mice contained $CD11c^+$ DCs expressing high levels of CD40 ($CD40^{hi}$) as a sign of maturity. This was not observed in mesenteric lymph nodes or spleen, whereas DCs expressing low levels of CD40 ($CD40^{low}$) were found in all three organs (Fig. 1A). Consequently, only $CD40^{hi}$ DCs but not $CD40^{low}$ DCs expressed the lymph node homing receptor CCR7 on their surface (Fig. 1B). Also, in agreement with previous findings [14, 24], $CCR7^{-/-}$ mice showed smaller lymph nodes (Supporting Information. Fig. 1). The CD103 marker has been used to identify tolerogenic, Tregs-converting DCs in the mesenteric lymph nodes and lamina propria [10, 25]. We found similar proportions of CD103 expression by both resident $CD40^{low}$ and migratory $CD40^{hi}$ DC subsets (Supporting Information Fig. 2).

Steady-state and immunogenic migratory DCs show different maturation stages

It is under debate how tolerogenic antigen uptake and presentation of self-antigens by DCs are handled during infections. To investigate how steady-state migratory DCs might be influenced under inflammatory conditions, we compared their surface profiles of MHC II, CD80 and CD86 with migratory DCs that have been matured by FITC-painting, known to induce contact hypersensitivity responses. After 1 day, FITC was detected transiently until day 6 in a fraction of $CD40^{hi}$ migratory DCs but not in $CD40^{low}$ resident DCs, suggesting that the hapten was transported from the skin to the draining lymph nodes by $CD40^{hi}$ migratory DCs. In the same lymph node $CD40^{hi}$ $FITC^-$ DCs, representing steady-state migratory DCs, were also constantly present throughout the sensitization phase (Fig. 2). Interestingly, the steady-state migratory DCs retained their partially mature phenotype during sensitization, while the $FITC^+$ migratory DC fraction expressed transiently much higher levels of CD86, CD80 and MHC II molecules (Fig. 2 and Supporting Information Fig. 3). These findings support the concept that two different maturation stages of DCs can migrate in parallel to provide steady-state and inflammatory/pathogen-derived antigen transport.

© 2011 WILEY-VCH Verlag GmbH & Co. KGaA, Weinheim

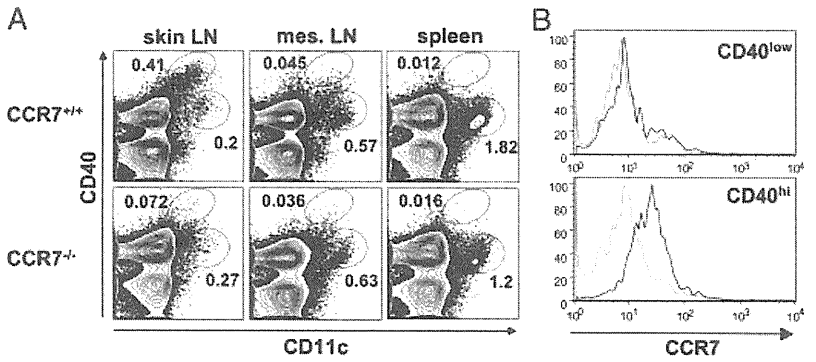

Figure 1. Characterization of steady-state migratory and resident DCs. (A) Cells from skin-draining or mesenteric lymph nodes and spleen of WT or CCR7$^{-/-}$ mice were stained with CD11c and CD40. The contour plots shown represent cells within an FSC/SSC gate for live cells. Dead cells were excluded by DAPI staining. Migratory and resident DCs in the skin-draining lymph nodes were detected as CD40^{hi} and CD40^{low} populations (oval gates), respectively. (B) CCR7 (black lines) was expressed on CD11c^{+} CD40^{hi} migratory DCs in peripheral lymph nodes but absent on the CD11c^{+} CD40^{low} population. Isotype control stainings are overlayed (gray lines). Each figure shows one representative result of at least two experiments.

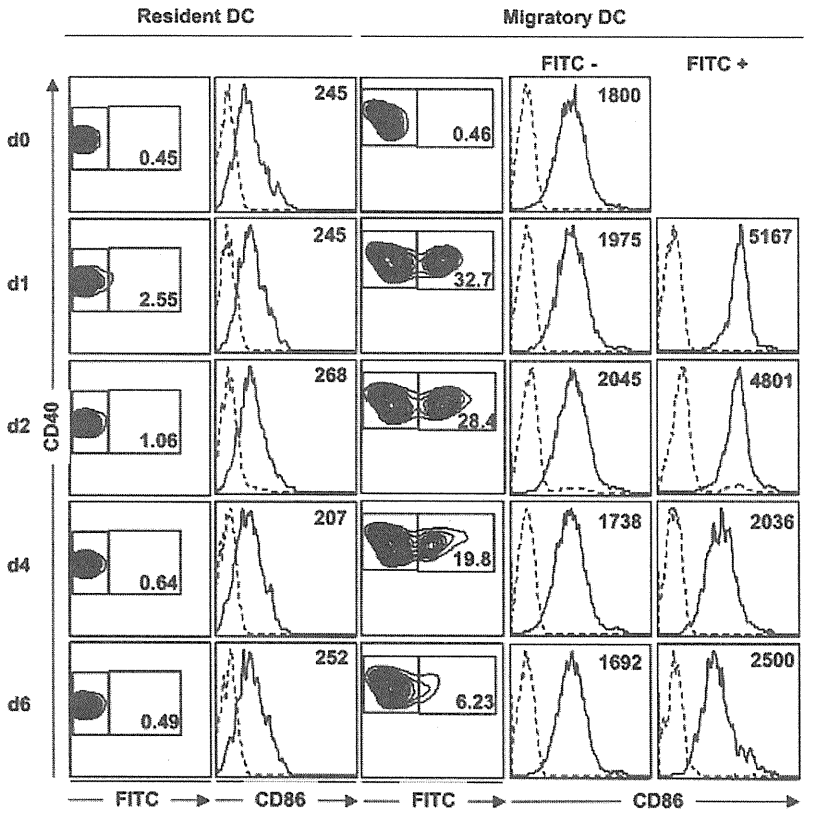

Figure 2. In vivo activation of skin DCs by skin sensitizing reveals an intermediate maturation phenotype of steady-state migratory DCs. The kinetics of FITC expression of migratory and non-migratory DCs in the skin draining lymph nodes of FITC painted mice is shown as contour plots stained against their CD40^{hi} or CD40^{low} expression. Skin-draining lymph nodes were isolated from mice at 0–6 days after FITC painting on the abdomen. Histograms show the CD86 (straight lines) or isotype stainings (dotted lines) on FITC^{-} resident DCs (left panel). The CD86 expression of CD40^{hi} migratory DC is shown separately within gates for FITC^{-} or FITC^{+} cells. MFIs are indicated in histograms. Percentages of FITC^{+} cells are indicated within the contour plot gates. Data are representative of three independent experiments.

Steady-state migratory CD40^{hi} DC express RelB, which is translocated into the nucleus

Within the Rel/NF-κB transcription factor family, tissue-specific and inducible members have been described. Since RelB was identified as the constitutively active κB-binding activity in lymphoid tissues under steady-state conditions [26], we investigated expression levels and subcellular distribution of RelB in sorted DC subsets. Analyses of peripheral lymph node DCs revealed that only the CD11c^{+} CD40^{hi} migratory DCs expressed

© 2011 WILEY-VCH Verlag GmbH & Co. KGaA, Weinheim

intracellular RelB (Fig. 3A). This expression was equally strong in EpCAM^{hi} DCs, which represent epidermal LC and langerin^{+} dermal DC subsets [22], and EpCAM^{low} DCs, reported to be langerin^{-} dermal DCs [22], but was not restricted to CD103^{+} DCs that represent a cross-tolerizing DC subtype [21] (Fig. 3B). Thus, steady-state migration of DCs correlates with RelB expression but not with a specific skin DC subset.

When the intracellular distribution of RelB was determined by confocal microscopy only very low levels of RelB were detected in the cytoplasm of resident DCs, but RelB expression was increased in steady-state migratory DCs. A substantial amount localized to the nucleus, similar to what we observed for FITC^{-} DCs of contact-sensitized mice, which represent steady-state migratory DCs under FITC treatment (Fig. 3C and Supporting Information Fig. 4). In FITC^{+} DCs RelB expression in the nuclei remained high. In contrast, c-Rel could not be detected in the nuclei of resident, steady-state migratory, FITC^{-} or FITC^{+} DCs, while nuclear RelA (p65) staining appeared in all four subsets (Fig. 3C and Supporting Information Fig. 4). Thus, nuclear translocation of RelB is observed not only under immunogenic conditions but also in migratory DCs during the steady state.

We then asked whether nuclear RelB is of functional relevance for the appearance of steady-state migratory DCs in the lymph nodes. Since homozygous RelB-deficient mice lack lymph nodes [27], we tested heterozygous *relB*$^{+/-}$ mice for their proportions of DC subsets in peripheral lymph nodes. Although lymph nodes from *relB*$^{+/-}$ mice appeared to be slightly smaller than their WT counterparts, the relative number of resident CD40^{low} DCs remained unchanged whereas the frequency of steady-state migratory CD40^{hi} DCs was significantly decreased within *relB*$^{+/-}$ skin-draining lymph nodes (Fig. 3D). To further confirm a specific role of the alternative NF-κB pathway, the RelB-binding partner p52 was investigated. The lymph nodes of *p52*$^{-/-}$ mice were much smaller than those of WT or *p50*$^{-/-}$ mice (Fig. 3E)

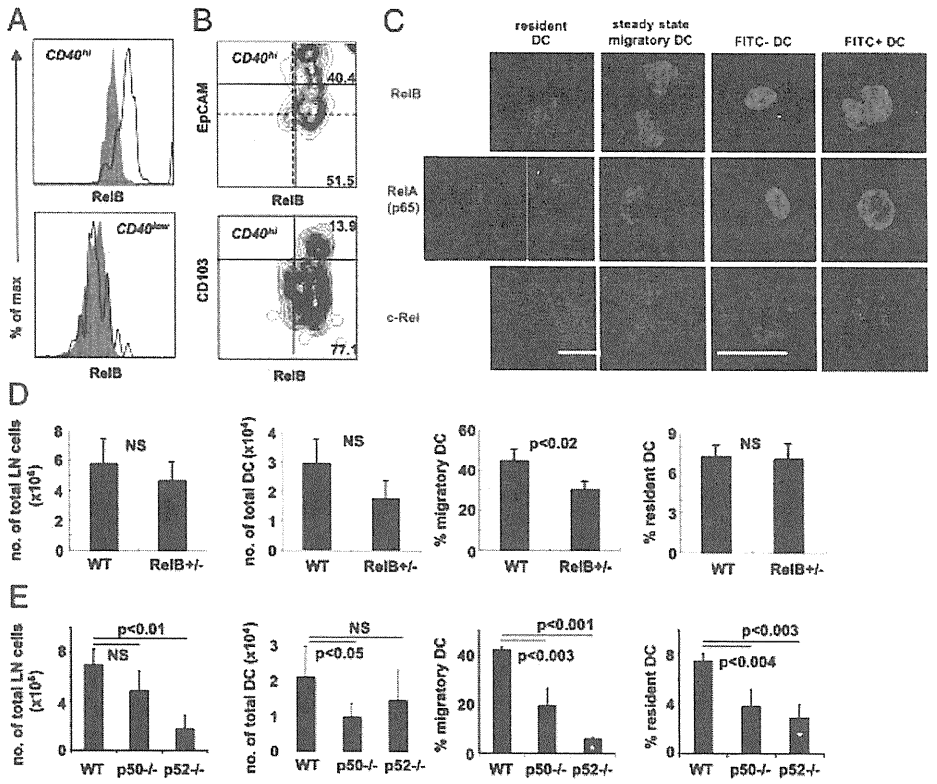

Figure 3. Steady-state migratory DCs show nuclear translocation of RelB and selectively decreased percentages in *relB*$^{+/-}$ and *p52*$^{-/-}$ mice. (A) Steady-state migratory DCs from peripheral lymph nodes were stained for CD11c, CD40 and intracellular RelB. Histograms show RelB expression (black line) as compared to isotype control stainings (filled gray) in CD40^{hi} steady-state migratory DCs (upper histograms) or CD40^{low} resident DCs (lower histograms). (B) CD11c^{+} CD40^{hi} steady-state migratory DCs from peripheral lymph nodes were additionally stained for intracellular RelB and surface EpCAM or CD103. For the EpCAM dot plot, different quadrants were set according to isotype control stainings (dotted lines) or to calculate the statistics (black lines). (C) Inflammation-induced migratory DCs (CD40^{hi} FITC^{+}), steady-state migratory DCs under inflammatory conditions (CD40^{hi} FITC^{-}), steady-state migratory CD40^{hi} DCs from untreated mice and resident CD40^{low} CD11c^{+} DCs were isolated from skin-draining lymph nodes by flow cytometric cell sorting (purity >95%) from skin-draining lymph nodes of mice 2 days after FITC painting. Cytospin preparations of cells were stained for DAPI and RelB, RelA or c-Rel. Scale bar, 5 μm. (D) Peripheral lymph nodes of WT ($n = 5$) and *relB*$^{+/-}$ mice ($n = 5$) or (E) WT ($n = 4$), *p50*$^{-/-}$ ($n = 4$) and *p52*$^{-/-}$ mice ($n = 4$) were isolated and single-cell suspensions compared for their total cell numbers and the proportions of CD11c^{+} CD40^{hi} migratory and CD11c^{+} CD40^{low} resident DCs within a FSC/SSC gate for large cells, i.e. largely excluding lymphocytes. Error bars indicate standard deviations analyzing individual mice. Statistical analyses using the paired Student's t-test are shown (NS = not significant). Bars marked with white asterisks indicate normalization to specific B-cell deficits in p52$^{-/-}$ mice

© 2011 WILEY-VCH Verlag GmbH & Co. KGaA, Weinheim

due to a known specific loss of $B220^+$ B cells in these mice [28]. Peripheral lymph nodes of $p52^{-/-}$ mice showed a dramatic reduction in the frequency of migratory but only partial effects on resident DCs (Fig. 3E). To investigate whether the classical NF-κB pathway through RelA/p50 would contribute to steady-state DC migration, we analyzed $p50^{-/-}$ mice. The binding partner RelA could not be screened this way since $relA^{-/-}$ mice die at the embryonic stage [27]. Peripheral lymph nodes of $p50^{-/-}$ mice showed equally reduced numbers of resident and migratory DCs. This indicates that p50 affects DCs at the immature stage but this defect is not enhanced upon partial maturation as observed for the steady-state migratory DCs (Fig. 3E). Thus, activation of the alternative NF-κB pathway through RelB/p52 correlated with the partial maturation state of DCs and was required for a normal frequency of steady-state migratory DCs in skin-draining lymph nodes.

Only migratory DCs transport and present epidermal OVA

K5-mOVA transgenic mice express membrane-bound (cell-associated) OVA in epidermal keratinocytes as well as in epithelial cells within the thymus and esophagus under the control of the keratin-5 promoter [29]. Recently, we reported that the epidermal neo-self-antigen OVA was transported and cross-presented in K5-mOVA mice by migratory DCs into skin-draining lymph nodes leading to deletion of OVA-specific OT-I $CD8^+$ T cells [30]. To investigate which populations within peripheral lymph nodes were able to present OVA to $CD4^+$ T cells we sorted $CD11c^+$ and $CD11c^-$ cells prom peripheral lymph nodes of K5-mOVA WT mice or crossed with $CCR7^{-/-}$ mice in which migratory DCs are missing. The different DCs were then cultured with BO97 OVA-specific hybridoma T cells. The results indicated that BO97 cells only responded to $CD11c^+$ cells from mice containing migratory DCs and mice heterozygous for CCR7 show intermediate responses (Fig. 4A). Then resident $CD40^{low}$ or migratory $CD40^{high}$ expressing $CD11c^+$ DCs from peripheral lymph nodes of K5-mOVA mice were cultured with BO97 cells. While resident DCs could not stimulate the BO97 cells, migratory DCs were able to present OVA (Fig. 4B).

We further investigated whether DCs from skin-draining lymph nodes of K5-mOVA mice would also stimulate fresh OVA-specific $CD4^+$ T cells. Migratory $CD40^{hi}$ and resident $CD40^{low}$ DCs were sorted from pooled skin-draining lymph nodes of either K5-mOVA or WT mice. These DCs were incubated with anti-CD40 and LPS to achieve full maturation and with either purified $CD4^+$ OT-II × RAG-$1^{-/-}$ or $CD8^+$ OT-I T cells. After 60 h, OVA-specific responses of $CD4^+$ or $CD8^+$ T cells were detected only by steady-state migratory $CD40^{hi}$ DCs from K5-mOVA mice but not with $CD40^{low}$ DCs from K5-mOVA mice or DCs from WT controls (Fig. 4C). While cell division of OT-I cells was low but readily detectable, OT-II cells showed clear CD69 but little CD25 upregulation and the proliferation remained very low (Fig. 4C). Thus, in vitro steady-state migratory DCs but not resident DCs contained low amounts of endogenous OVA. The transported epidermal self-antigen OVA allowed substantial cross-presentation but hardly conventional MHC II presentation. Importantly, resident DCs could not present or cross-present OVA under steady-state conditions, ruling out transfer from migratory to resident DC subtypes.

Steady-state migratory DCs mediate Treg conversion in vitro by using endogenous TGF-β

To address whether OT-II cell activation by steady-state migratory DCs would enable TGF-β-dependent Treg conversion, the differential DC subsets were first stained on their surface for the TGF-β-associated molecule latency-associated peptide (LAP), which has been shown to correlate with Treg conversion by human DCs [31]. The highest expression was found on $CD40^{high}$ DCs, while it was lower on $CD40^{low}$ DCs both from peripheral lymph nodes and at intermediate levels on $CD11c^+$ DCs from mesenteric lymph nodes (Fig. 5A). To test whether this differential LAP expression would reflect different Treg conversion rates, in vitro co-cultures of WT DCs and purified $CD4^+$ $CD25^-$ OT-II cells in the presence of OVA were performed for 5 days and then tested for CD25 and Foxp3 expression. While all conditions led to CD25 upregulation, only $CD40^{high}$ DCs showed a substantial conversion that could be blocked by anti-TGF-β (Fig. 5B). Resident $CD40^{low}$ DCs were unable to generate $Foxp3^+$ cells, but addition of exogenous TGF-β allowed some $Foxp3^+$ Treg induction (Fig. 5B). Total $CD11c^+$ DCs from mesenteric lymph nodes were similarly able to perform this in vitro conversion (data not shown) as reported before [10]. Addition of exogenous porcine TGF-β did not further increase the conversion rate of $CD40^{high}$ DCs but rather seemed to compete with the endogenous TGF-β, leading to lower conversion rates.

Thus, steady-state migratory DCs but not lymph node resident DCs have the capacity to convert $CD4^+$ T cells into Tregs by using endogenous TGF-β/LAP complexes on their surface.

Treg conversion in vivo occurs through langerin$^+$ dermal DCs

The minipump system was used before to show Treg conversion in vivo [5]. To investigate whether steady-state migratory DCs can transport and present soluble self-antigen to T cells in vivo also in our system, we transferred $CFSE^+$ OVA-specific transgenic OT-II cells into mice implanted with an osmotic minipump secreting continuously low amounts of $OVA_{327-339}$ peptide. Activated $CD4^+$ $CD25^+$ $Foxp3^-$ and $CD4^+$ $CD25^+$ $Foxp3^+$ Tregs of OT-II origin accumulated in the skin-draining lymph nodes of OVA peptide pump-implanted mice similarly as described before [5]. Control mice implanted with a PBS pump accumulated neither activated nor regulatory OT-II T cells (Fig. 6A, upper row).

© 2011 WILEY-VCH Verlag GmbH & Co. KGaA, Weinheim

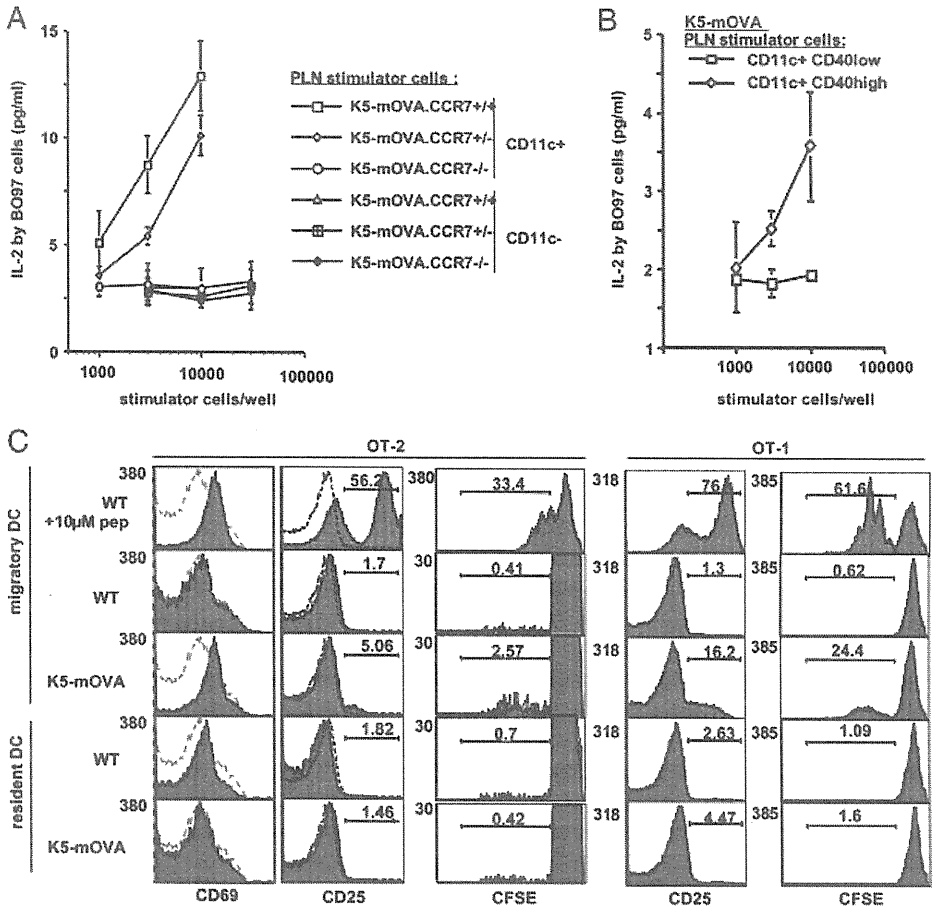

Figure 4. Low levels of epidermal self-antigen are presented and cross-presented in vitro only by migratory DCs isolated from K5-mOVA mice. (A) $CD11c^+$ or $CD11c^-$ cells or (B) migratory $CD11c^+$ $CD40^{hi}$ or resident $CD11c^+$ $CD40^{low}$ DCs from peripheral lymph nodes (PLN) of the indicated mice were enriched and cultured with OVA-specific BO97 hybridoma T cells. T-cell responses were measured as IL-2 production. (C) $CD11c^+$ $CD40^{hi}$ or $CD11c^+$ $CD40^{low}$ DCs were sorted from skin-draining lymph nodes of WT or K5-mOVA mice by flow cytometry (purity >93%). $CD8^+$ OT-I T cells and $CD4^+$ OT-II × RAG-$1^{-/-}$ T cells were purified by magnetic cell sorting (purity >90%) and labeled with CFSE. In total, 3×10^4 DCs, LPS, anti-CD40 and T cells were mixed at a 1:1 ratio and cultured for 60 h. As a positive control, $OVA_{257-264}$ or $OVA_{327-339}$ peptides were added to cultures of $CD11c^+$ $CD40^{hi}$ DCs from WT mice with OT-I or OT-II × $RAG1^{-/-}$ cells, respectively. CFSE dilution, CD69 and CD25 expressions are shown as histograms. Dotted overlays represent stainings of unstimlated OT-II cells. Percentages indicate dividing or activated populations, respectively. All experiments were performed three times with similar results.

Moreover, K5-mOVA mice that received OT-II cells for the same period of time presented cell-associated self-antigens in skin-draining lymph nodes as indicated by the appearance of activated $CD25^+$ $Foxp3^-$ and regulatory $CD25^+$ $Foxp3^+$ OT-II cells. To clarify whether activation and Treg induction in both systems was dependent on migratory DCs, OT-II cells were transferred into OVA peptide pump-implanted mice or K5-mOVA mice lacking CCR7, the chemokine receptor known to be required for DC migration to lymph nodes [14]. In the absence of migratory DCs in $CCR7^{-/-}$ mice, both activation and Treg induction were completely aborted (Fig. 6A, lower row). This suggests that low doses of soluble and cell-associated antigens require transport by DCs to draining lymph nodes to accumulate activated and Tregs.

To control whether fluid phase transport of antigen is intact in $CCR7^{-/-}$ mice, CFSE-labeled OT-II cells were transferred into $CCR7^{-/-}$ mice that were then injected s.c. with titrated amounts of $OVA_{327-339}$ peptide. In both WT and $CCR7^{-/-}$ mice OT-II cells proliferated dose-dependently, indicating an intact conduit system and antigen presentation by the resident DC subset in $CCR7^{-/-}$ mice (Supporting Information Fig. 5). The proliferation rates of OT-II cells were slightly reduced in $CCR7^{-/-}$ mice, which may reflect the contribution of migratory DCs to the antigen presentation in the lymph node.

The skin is populated by epidermal LCs and two subsets of $langerin^+$ and $langerin^-$ dermal DCs [18–20], which are all migratory and may transport antigens from osmotic pumps or cell-associated epidermal OVA in K5-mOVA mice. To test whether $langerin^+$ DCs were involved in the transport of keratinocyte-associated epidermal OVA, we crossed K5-mOVA mice with mice expressing the diphtheria toxin receptor (DTR) under the langerin promoter (langerin-DTR mice), which allows ablation of LCs and $langerin^+$ dermal DCs by diphtheria toxin injection [19].

© 2011 WILEY-VCH Verlag GmbH & Co. KGaA, Weinheim

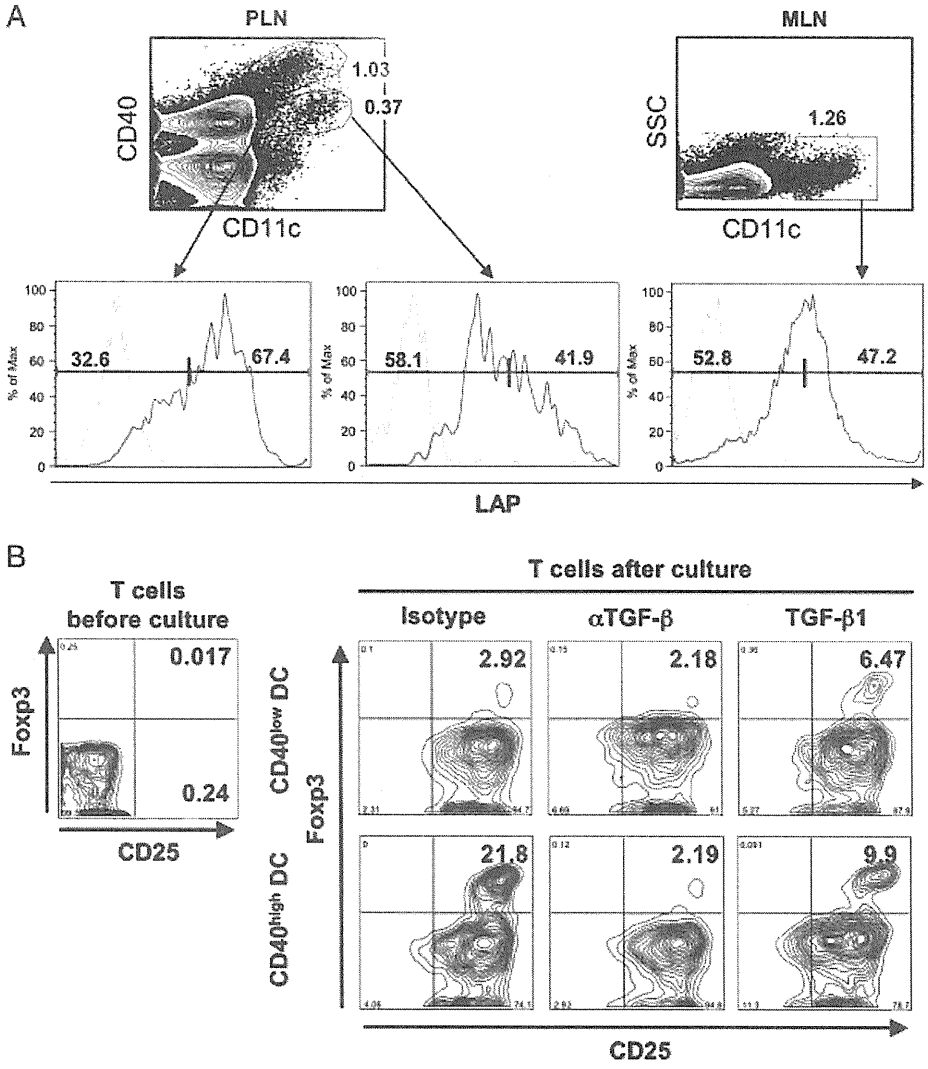

Figure 5. Steady-state migratory DCs express high levels of surface LAP and mediate Treg conversion in vitro by endogenous TGF-β. (A) DC were analyzed by flow cytometry from peripheral lymph nodes (PLN) or mesenteric lymph nodes (MLN) for their surface expression of CD11c, CD40 and LAP. Numbers indicate the percentages of cells within the indicated gates. Black line indicates LAP stainings and gray filled line the isotype controls. These experiments were performed two times with similar results. (B) FACS-sorted CD40^{high} steady-state migratory DCs or CD40^{low} resident DCs from skin-draining lymph nodes of WT mice were cocultured with CD4$^+$ CD25$^-$ OT-II T cells in the presence of OVA peptide. A blocking TGF-β antibody, isotype control antibody or recombinant TGF-β1 was added. Foxp3 and CD25 expression was analyzed at day 5. All dot plots were gated on CD4$^+$ Vβ5$^+$ cells. These experiments were performed four times with similar results.

Analysis of transferred OT-II cells in these mice showed no activation or Treg induction (Fig. 6B). These results indicate that migratory langerin$^+$ dermal DCs or LCs transport epidermal self-antigen to the lymph nodes.

To further discriminate between these two DC subtypes bone marrow chimera experiments were performed. K5-mOVA mice were irradiated and reconstituted with MHC II$^{-/-}$ bone marrow cells. In the skin of these mice only the radioresistant LCs remain MHC II$^+$ while both dermal DC subsets appear MHC II$^-$ (Supporting Information Fig. 6). Transfer of OT-II cells into these chimeras abrogated Vβ5$^+$ OT-II cell proliferation and their conversion into Foxp3$^+$ Tregs whereas WT chimeras remained unaffected (Fig. 6C). Thus, only the langerin$^+$ dermal DC subset appears competent for Treg appearance in K5-mOVA mice. These data are consistent with findings that OVA cross-presentation to CD8$^+$ OT-I cells in K5-mOVA mice is also performed by this DC subset [21, 22].

Steady-state migratory DCs induce naive T-cell conversion, expansion and regulation of Tregs

In the previous experiments bulk OT-II cells were adoptively transferred, which contained both naive conventional CD4$^+$ T cells and Treg. To determine whether the appearance of CD4$^+$ CD25$^+$ Foxp3$^+$ OT-II Tregs in peripheral lymph nodes from

© 2011 WILEY-VCH Verlag GmbH & Co. KGaA, Weinheim

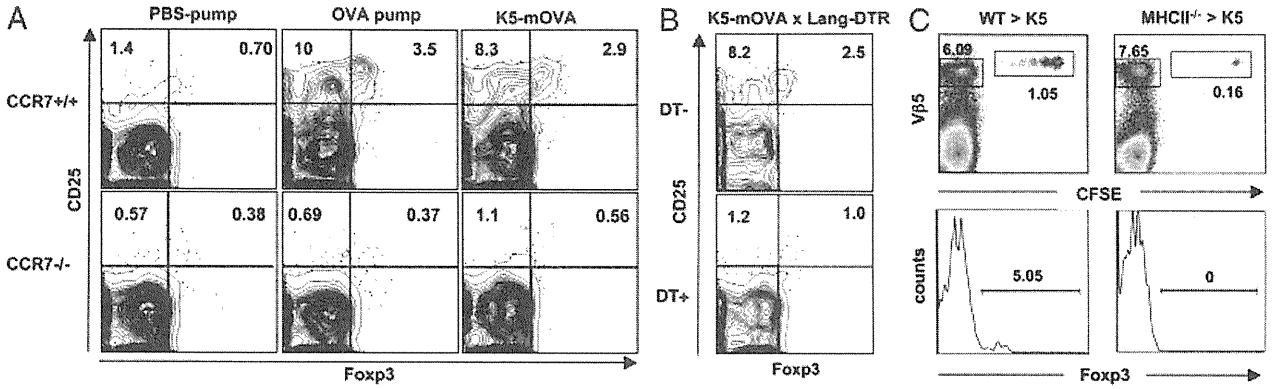

Figure 6. Treg conversion in the draining lymph node requires migratory langerin$^+$ dermal DCs. (A) CFSE-labeled bulk OT-II lymph node and spleen cells (3×10^7) were transferred into mice implanted under the skin with a PBS-loaded or $OVA_{327-339}$ peptide-loaded pump or into K5-mOVA mice. Dot plots shown in the upper and lower rows indicate whether these mice were on a WT CCR7$^{+/+}$ or CCR7$^{-/-}$ background, respectively. The osmotic pumps were implanted 2 days before OT-II cell transfer. Thirteen days after adoptive transfer, mice were sacrificed and the skin-draining lymph nodes were removed to perform FACS analysis. Contour plots show surface CD25 and intracellular Foxp3 expression of CD4$^+$ CFSE$^+$ cells. (B) Migratory langerin$^+$ cells are required to induce CD25$^+$ Foxp3$^+$ Tregs to epidermal cell-associated antigen. CFSE-labeled bulk OT-II lymph node and spleen cells (3×10^7) were transferred into K5-mOVA × langerin-DTR mice (DT–). To ablate LCs in these mice, 1 μg diphtheria toxin was injected at days −7, 0 and 7 (DT+). (C) K5-mOVA mice were irradiated and reconstituted with WT or MHC II$^{-/-}$ bone marrow and CD4$^+$ CD25$^-$ OT-II cells were transferred to follow their proliferation of transgenic Vβ5$^+$ cells. Foxp3 expression was detected 13 days after transfer. Displayed cells are gated for CD4$^+$ Vβ5$^+$. Percentages of cells are indicated within the quadrants or gates. The experiments are representative of four and two experiments with similar results.

K5-mOVA mice was due to the trapping or expansion of pre-existing Tregs or due to peripheral conversion of naive T cells, we used purified CD4$^+$ T cells from OT-II × RAG-1$^{-/-}$ mice for the adoptive transfer into K5-mOVA mice. In OT-II mice on a RAG-deficient background only naive conventional CD4$^+$ T cells were released from the thymus but not Foxp3$^+$ Tregs (Supporting Information Fig. 7). Analysis of skin-draining and mesenteric lymph nodes as well as the spleen indicated that after 13 days CD4$^+$ CD25$^+$ Foxp3$^+$ Tregs appeared predominantly in peripheral lymph nodes (Fig. 7A). Since the adoptively transferred cells were also labeled with CFSE, we were able to follow their proliferation. Analysis of the CD4$^+$ CFSE$^+$ population indicated that these cells clearly divided and, among those, the proportion of CD25$^+$ Foxp3$^+$ cells was higher in dividing than non-dividing cells (Fig. 7B). Although expression of Foxp3 in murine CD4$^+$ T cells is strictly linked to functional suppression, the regulatory capacity of induced OT-II Tregs was tested by OVA injection into WT or K5-mOVA mice that were either adoptively transferred by CD25$^-$ OT-II cells 10 days before to allow their Treg conversion or were left untreated. Then, CFSE-labeled CD25$^-$ OT-II responder cells were transferred into all mice at the day of OVA-injection. The proliferative capacity of the CFSE$^+$ OT-II responder cells was inhibited in WT mice by 18%, most likely due to the activity of CD4$^+$ CD25$^-$ Foxp3$^+$ Tregs that have been transferred (data not shown). The inhibition of proliferation in K5-mOVA mice was clearly higher by 30%, indicating an increased regulatory activity (Fig. 7C). These data suggest that conversion of naive CD4$^+$ OT-II cells into 2–3% proliferating Tregs by steady-state migratory DCs that could be observed after 14 days in the draining lymph nodes of K5-mOVA mice led almost to a doubling in the suppressive capacity from 18 to 30% within the same time period.

Discussion

Immature DCs and CD4$^+$ CD25$^+$ Foxp3$^+$ Tregs represent major tolerogenic immune cells [32–34]. Therefore, immature DCs were also believed to be major interaction partners and inducers of Tregs [12, 35]. However, for Treg homeostasis CD28 costimulation is required [7], which cannot be provided by immature DCs. Mature DCs highly express costimulatory molecules but mainly act immunogenic [32]. Surprisingly, mature DCs have also been shown to be superior to immature DCs in the expansion of pre-formed Tregs in mice [36–39]. It remained unclear, however, which DC maturation stage was responsible for conversion of naive CD4$^+$ T cells into Foxp3$^+$ Tregs under steady-state conditions in vivo. We and others proposed earlier that a semi-mature DC stage, such as after stimulation with TNF or E-cadherin disruption, may lead to optimal induction of Foxp3$^-$ IL-10$^+$ T cells [13, 40, 41]. For human thymic "more mature" DCs the conversion into Foxp3$^+$ Tregs has been shown [42]. Thus, a certain extent of DC maturation but not immature DCs may induce de novo Treg conversion under physiological conditions.

Here we showed that steady-state migratory DCs in peripheral lymph nodes display a semi-mature DC phenotype, characterized by intermediate surface expression of MHC II, CD80, CD86, CD40, nuclear RelB and surface LAP/TGF-β complexes. Functionally they transport CCR7-dependent peripheral self-antigens to the draining lymph nodes and present them with some costimulation. They convert naive CD4$^+$ T cells into Tregs. In the case of cell-associated epidermal OVA, the langerin$^+$ dermal DC subset was required to mediate this effect.

Several authors observed that peripheral lymph nodes of mice contain a fraction of mature CD40^{hi} DCs [14, 43–45]. Here steady-

© 2011 WILEY-VCH Verlag GmbH & Co. KGaA, Weinheim

state migratory DCs already show nuclear activity of RelB but have only a partially mature phenotype since costimulatory molecule expression on FITC$^+$ DCs was still higher. Our data suggest that nuclear activity of RelB and p52 are needed for inducing or maintaining the phenotype of the steady-state migratory DCs. RelB has previously been described to be expressed in the T-cell areas of lymph nodes [46]. RelB-deficient mice lack peripheral lymph nodes and the CD8α^{neg} myeloid DC lineage, indicating that this transcription factor is important for organogenesis of certain secondary lymphoid organs and myeloid DC development [47, 48]. These mice also develop T-cell-dependent multi-organ inflammation, which further points to a role of RelB as an anti-inflammatory factor in the steady state [49]. RelB may bind to its partner p52, since the *p52*$^{-/-}$ mice also showed a severe reduction of migratory DCs. In contrast, *p50*$^{-/-}$ mice displayed no specific effect on migratory DCs and both resident and migratory DC populations of the peripheral lymph nodes were equally affected. This points to a role of p50 already at the immature DC stage since the effect was not further increased after maturation into steady-state migratory DCs. Together, our data suggest that steady-state migratory DCs partially depend on the alternative NF-κB pathway, mediated through RelB/p52, whereas inflammatory DC maturation may occur through the classical NF-κB pathway as suggested by the requirement of p50 for IL-12p70 and c-Rel for IL-27 production by DCs [50, 51].

Naturally occurring Tregs, which develop in the thymus, play a major role for the maintenance of peripheral tolerance. However, peripherally induced Tregs have been reported only recently. The chronic delivery of peptides by implantation of osmotic pumps led to de novo induction of Tregs in the pump-draining peripheral lymph nodes after 2 wk [5]. Also targeting the DC receptor DEC205 but not 33D1 of splenic DCs induced Foxp3$^+$ Tregs in the steady state in vivo [9]. In models of oral tolerance, it was shown that a population of CD103$^+$ DCs isolated from mesenteric lymph nodes [10] mediated Treg conversion in vitro. Similarly, a CD103$^+$ DC was identified in the lamina propria to mediate Treg conversion in vitro or under lymphopenic conditions in vivo [25]. Since exogenous peptide or anti-CD3 had to be added to demonstrate Treg conversion, it remained unclear whether these DCs could transport orally administered antigens from the gut to mesenteric lymph nodes or lamina propria. In skin-draining lymph nodes CD103$^-$ DCs were responsible for Treg conversion in vitro [52]. In vivo Treg conversion data for a skin-derived self-antigen are still lacking. We found similar CD103 levels on a subpopulation (~20%) of migratory and resident DCs from peripheral or mesenteric lymph nodes, suggesting that this marker may not generally serve to identify CCR7$^+$ migratory DCs with the ability to transport self-antigens and convert Tregs. Comparing the efficiency of CD4$^+$ T-cell activation and Treg conversion in vitro by exogenously added peptide or in vivo by endogenous OVA from the DCs it appears that the in vitro and in vivo response to endogenous OVA is rather low. The poor efficacy of Treg conversion in our system may reflect the physiological situation where only small amounts of self-antigens are presented by few steady-state migratory DCs. It is of note that our system only relies on endogenous antigen, and not high doses of orally applied OVA, lymphopenic conditions or antibody targeting. The OVA pump control experiments and in vitro Treg conversion rates showed a poor Foxp3$^+$ Treg induction, which may also indicate an intrinsically poor capacity of the OT-II TCR to be activated/converted in this system.

We found that besides Treg conversion also a substantial activation of conventional T cells occurred, appearing as a CD4$^+$ CD25$^+$ Foxp3$^-$ subset. This was not observed by others using the same minipump system but different TCR-transgenic T cells [5]. We cannot explain the differential behavior of the transgenic T cells but the activated conventional T cells in our system may produce IL-2 and thus explain the proliferation of Tregs.

Treg conversion requires TGF-β to induce the transcription factor Foxp3 and retinoic acid counteracts costimulation on the converting APCs [8, 10, 53]. Our data indicate that steady-state migratory but not resident DCs of peripheral lymph nodes directly activate naive CD4$^+$ T cells and use endogenous TGF-β for Treg conversion, which was detectable by LAP staining at the cell surface, similar as described for splenic CD8α$^+$ DEC205$^+$ DCs ex vivo [54] or by in vivo targeting to DEC205 [9, 55]. However, a contribution of splenic DCs to the repertoire of peripherally induced Tregs remains to be shown. Although successful antibody targeting of DEC205 has been shown for all three skin DC subsets [56] and this pathway opens a wide array of therapeutical implications [57], physiological ligands of this receptor and its contribution for tolerance induction are not known. Whether the TGF-β is produced by the DC itself or captured form environmental sources such as shown for intestinal epithelial cells remains open [58]. Although we tested retinoic acid inhibitors our results remained unclear and require further investigations, since retinoic acid can also be produced by epithelia [58].

It has been shown that CD80/86 costimulation by DCs counteracts Treg conversion and therefore suppression of CD80/86 expression by retinoic acid may favor DC immaturity and thereby Treg conversion [8, 54]. In contrast, in vitro conversion stimulated through antibodies instead of APCs requires also CD28 antibodies in conjunction with anti-CD3 and TGF-β [59], indicating that some CD80/86 costimulation may be required or it can be substituted by other molecules expressed on DCs such as PD-L1 or GITR [54]. DCs also needed to express CD80/CD86 to convert Tregs efficiently in vitro by using splenic DC subsets because this costimulation induced conventional T cells to produce IL-2, which was required for the conversion [39, 60]. Our data suggest that the semi-mature phenotype of steady-state migratory DCs provides endogenous TGF-β, detected as LAP on their surface, and an intermediate optimal dose of CD80/86 for Treg conversion.

One would expect that epidermal LCs in K5-mOVA mice capture epidermal cell-associated OVA antigen much better than dermal DCs. However, we did not observe Treg induction in draining lymph nodes from bone marrow chimeric mice in which only radioresistant LCs remained capable of MHC II presentation to OT-II cells. The results from K5-mOVA × langerin-DTR mice, where both epidermal LCs and langerin$^+$ dermal DCs were

© 2011 WILEY-VCH Verlag GmbH & Co. KGaA, Weinheim

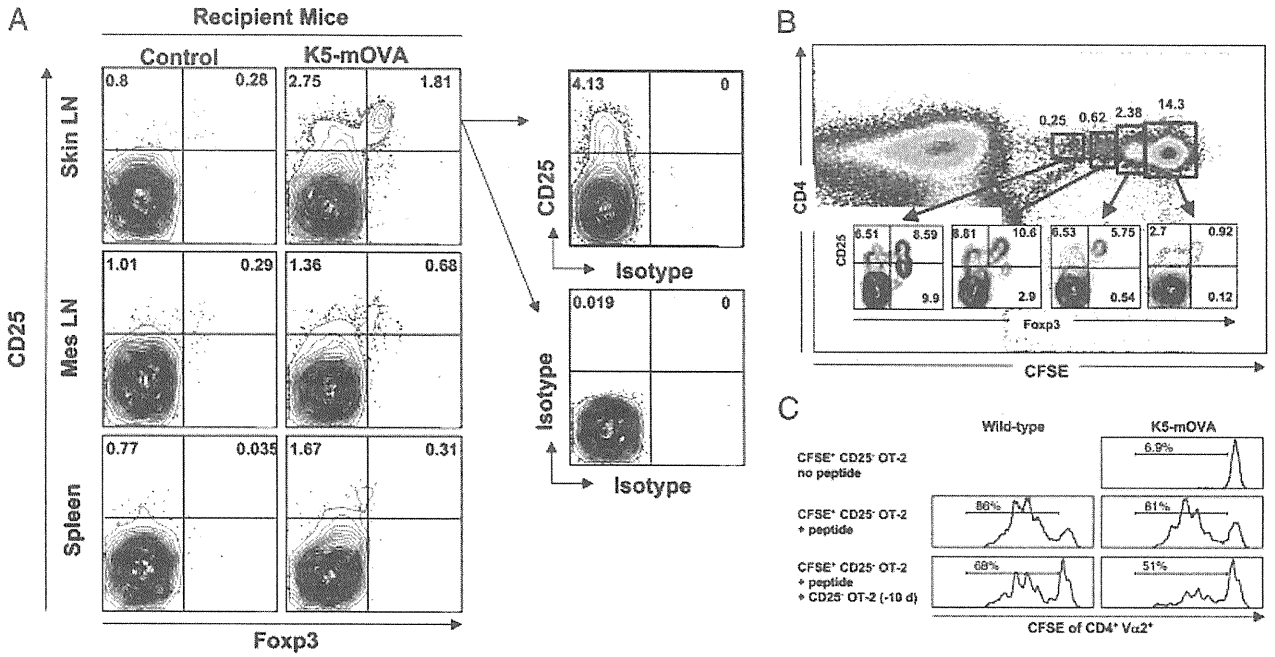

Figure 7. De novo induction, proliferation and suppressor activity of CD25$^+$ Foxp3$^+$ Tregs in K5-mOVA mice. CFSE-labeled purified CD4$^+$ T cells from OT-II × RAG-1$^{-/-}$ mice (9×10^6) were transferred into mice expressing no OVA (control) and into K5-mOVA mice on OT-II transgenic background. After 13 days, the spleen, skin-draining and mesenteric lymph nodes were analyzed by FACS. Contour plots show surface CD25 and intracellular Foxp3 expression on CD4$^+$ CFSE$^+$ cells. Percentages of CD25$^+$ Foxp3$^-$ and CD25$^+$ Foxp3$^+$ cells are indicated in the quadrants. Related isoytpe stainings are shown in the right column. (B) Proliferation of OT-II × RAG-1$^{-/-}$ cells measured as CFSE dilution of CD4$^+$ cells. Inserted contour plots show activated CD25$^+$ Foxp3$^-$ and CD25$^+$ Foxp3$^+$ Treg fractions of dividing and non-dividing cells. Numbers above gates and within quadrants indicate the respective percentages. (C) Increased OVA-specific suppressor activity in K5-mOVA mice as compared to WT mice. WT or K5-mOVA mice were injected i.v. with 6×10^6 OT-II cells or remained untreated. After 10 days all mice were injected with 2×10^6 CFSE$^+$ CD25$^-$ OT-II responder cells and immunized with OVA peptide. Three days later the CFSE-dilution of the CD4$^+$ Vα2$^+$ OT-II responder cells in peripheral lymph nodes was measured by flow cytometry. The experiments are representative of three experiments with similar results.

depleted, provide strong evidence that steady-state migratory langerin$^+$ dermal DCs represent the major responsible DC population for OVA transport and presentation in our system. Similar data were obtained for the induction of cross-tolerance in K5-mOVA mice [21, 22], although a minor role for cross-presentation by LCs could not be fully excluded in other experimental settings. When OVA-specific CD8$^+$ OT-I T cells were transferred into LC-ablated K5-mOVA mice they still proliferated, indicating that epidermal self-antigen was transported and cross-presented by both LCs and dermal DCs in the skin-draining lymph node [30] (and data not shown). Models of how dermal DCs may access epidermal antigens are discussed elsewhere [15].

After adoptive transfer of TCR-transgenic Tregs their proliferation could be observed in lymph nodes draining the immunization site with mature DCs or adjuvant [60–62]. However, in situations where Treg induction was followed under steady-state conditions, as s.c. installed osmotic pumps, proliferation of Tregs has not been reported [5]. Here, we found that transgenic OVA that was transported by steady-state migratory DCs not only converted naive CD4$^+$ T cells into Tregs, but also stimulated their proliferation, although to a moderate extent of three to four divisions in 2 wk. Despite proliferation their suppressive potential was maintained and the proportion of Foxp3$^+$ cells was increasing with the number of cell divisions. Suppression of secondarily transferred OT-II cells was stronger in K5-mOVA mice than WT controls. Since we hardly observed proliferation of OT-II cells after implantation of OVA-secreting pumps (data not shown), proliferation of Tregs may be induced only by cell-associated but not by soluble antigens under steady-state conditions. By comparing directly the osmotic pump system with the K5-mOVA mice providing cell-associated antigens, we found a similar rate of Treg conversion in WT but not in CCR7$^{-/-}$ mice, which lack migratory DCs. The functionality of the reticular conduit system in CCR7$^{-/-}$ mice was shown by the presence of WT OT-II T cells in T-cell areas by OT-II cell proliferation after injection of high doses of soluble peptides. For very low doses of soluble antigen in the peripheral tissue, as provided by the pump system, transport by CCR7$^+$ migratory DC was required.

In conclusion, our data indicate that low levels of soluble or cell-associated neo-self-antigens in the skin require transport and presentation by CCR7$^+$ RelB$^+$ steady-state migratory DCs and cannot be mediated by fluid phase transport to immature lymph node-resident DCs. In K5-mOVA mice steady-state migratory langerin$^+$ dermal DCs are the major subset in converting adoptively transferred naive CD4$^+$ T cells into proliferating Foxp3-expressing Tregs. Only migratory but not resident DCs can mediate Treg conversion by endogenous TGF-β. Thus, we identified and characterized the antigen presenting cell type, which is

© 2011 WILEY-VCH Verlag GmbH & Co. KGaA, Weinheim

responsible for the de novo Treg induction under physiological conditions in skin-draining lymph nodes in vivo.

Materials and methods

Mice

All mice were bred and maintained at the Universities of Erlangen and Würzburg. K5-mOVA mice were obtained from Department of Dermatology, Osaka University [29]; and OT-I and OT-II mice were kindly provided by Francis Carbone, Melbourne, Australia. OT-II mice were crossed with RAG-1$^{-/-}$ mice (gifted from Thomas Winkler, Erlangen, Germany). CCR7$^{-/-}$ mice [24] and langerin-DTR-EGFP transgenic mice [63], each on a C57BL/6 background, were crossed with K5-mOVA. C57BL/6 and 129 mice were purchased from Charles River. MHC II$^{-/-}$ mice by Horst Bluethmann, F. Hoffmann-La Roche, Basel, Switzerland.

For bone marrow chimera experiments K5-mOVA mice were irradiated with two doses of 4.5 Gy each with an interval of 4 h. After another 4 h mice were reconstituted with 5×10^6 bone marrow cells from MHC II$^{-/-}$ or WT mice as a control. All animal experiments were performed in accordance with institutional guidelines and permission (Regierung von Unterfranken 55.2-2531.01-73/07) with age- and sex-matched animals.

Preparation and cell sorting of DCs from lymph nodes

Skin-draining lymph nodes (cervical, axillar, brachial and inguinal) were cut into small pieces and digested for 20 min at room temperature with 1 mg/mL DNase I (Sigma) and 1 mg/mL collagenase type III (Worthington) in RPMI 1640 containing 10% FCS, 50 μM 2-ME, 2 mM L-glutamine, 100 U/mL Penicillin (Sigma) and Streptomycin 100 μg/mL (Sigma). Lymph node tissue was then incubated in the same media for another 5 min at room temperature by adding 0.01 M EDTA to disrupt T cell–DC complexes. Then, the suspensions were passed through a 70 μm cell strainer to remove debris and cells were resuspended in PBS containing 5% FCS and 1 mM EDTA. From this step onwards, cells were always kept on ice or 4°C. Cells were stained with mAB against CD11c (HL-3) and CD40 (3.23). Cells were washed and resuspended in PBS containing 2% FCS, 1 mM EDTA and 1 μg/mL DAPI. CD40^{hi} and CD40^{low} cells from CD11c$^+$ DAPI$^-$ population were sorted with a MoFlo high-speed sorter (Cytomation).

Implantation of osmotic pumps secreting $OVA_{327-339}$ peptide

Osmotic minipumps (Alzet #1002) were filled with an $OVA_{327-339}$ peptide solution in PBS to secrete 10 μg/day for 14 days or PBS only, as previously described [5]. The pump was inserted into the s.c. cavity of recipient mice after a small incision in the back, and the wound was closed by the AUTOCLIP system (Becton Dickinson, BD). Two days after implantation, OT-II cells were adoptively transferred.

FACS analysis of DCs

Surface staining was performed using the following mAbs purchased from BD if not otherwise indicated: CD11c-FITC, -PE or -eFlour450 (eBioscience), CD40-biotin, -FITC or -APC (Miltenyi), CCR7-biotin (eBioscience), EpCAM-PE (eBioscience), CD103-biotin, MHC II-FITC or -PE, CD80-FITC, CD86-FITC, CD205 (Serotec), CD4-PE and CD8-PerCP and LAP-PE (R&D Systems). Biotinylated antibodies were detected by incubation with either PerCP- or APC-conjugated streptavidin (BD). As isotype controls the following fluorochrom-conjugated or biotinylated mAbs were used (all BD): mouse IgG1, rat IgG1, rat IgG2a, rat IgG2b, armenian hamster IgG2 and armenian hamster IgG1. Intracellular RelB staining (polyclonal rabbit IgG, Santa Cruz), was performed after 2% formaldehyde fixation and ice cold 90% methanol permeabilization. For detection a secondary goat-anti-rabbit IgG $F(ab)_2$ FITC-conjugate (Dianova) was used. Cells were measured with a FACSScan, FACSCalibur or FACSCanto II (BD) and analyzed with CellQuest (BD) or FlowJo software (Stanford University).

Adoptive transfer of OT-II cells

Cervical, axillary, brachial, inguinal and mesenteric lymph nodes and spleens were isolated from conventional OT-II or OT-II × RAG-1$^{-/-}$ mice and single-cell suspensions prepared. CD4$^+$ cells were enriched by using the "CD4 negative isolation kit" (purity >90%, Dynal). Briefly, cells were labeled with rat-anti-CD8, -CD11b, -CD16/32 (2.4G2), -CD45R (B220), -TER119 mAbs, followed by magnetic depletion with sheep-anti-rat Ig-Dynabeads conjugates (Dynal Biotech/Invitrogen). The untouched fraction was collected, and labeled with 5 μM CFSE (CFDA SE, Molecular Probes/Invitrogen) at 37°C for 10 min. Cells were washed with PBS and injected into the tail vein of recipient mice. After 3–13 days, recipient mice were sacrificed and cell suspensions were prepared from lymph nodes and spleen. Extracellular staining was performed using CD4-PerCP and CD25-APC mAbs (BD). Intracellular Foxp3 staining was conducted with the murine Foxp3-PE staining kit (eBioscience) following the manufactor's instructions. Isotype control stainings included the monoclonal rat IgG1-APC and rat IgG2a-PE (BD).

Immunization of mice with converted Tregs

K5-mOVA or WT control mice were left untreated or reconstituted with 6×10^6 CD4$^+$ CD25$^-$ OT-II cells. After 10 days all mice were adoptively transferred with 2×10^6 CFSE$^+$ CD4$^+$ CD25$^-$ OT-II cells and injected with 100 μg OVA peptide s.c. into the foot pads. Three days later the popliteal and inguinal lymph

© 2011 WILEY-VCH Verlag GmbH & Co. KGaA, Weinheim

nodes were removed and the single-cell suspension tested by FACS analysis for CD4, Vβ5 and CFSE.

In vitro Treg conversion assay

Naive $CD25^-$ $CD4^+$ T cells from lymph nodes and spleen of OT-II mice were separated using first a mouse $CD4^+$ T Cell Enrichment Kit ($CD4^+$ purity >90%, StemCells) and second CD25 MACS Micro Beads ($CD25^-$ $CD4^+$ purity >90%, Miltenyi). $CD40^{high}$ $CD11c^+$ and $CD40^{low}$ $CD11c^+$ DC from skin-draining lymph nodes were isolated and sorted as described above. A total of 20 000 $CD25^-$ $CD4^+$ OT-II T cells were cultured in round bottom 96-well plates with 6000 DCs for 5 days in the presence of 100 ng/mL $OVA_{327-339}$ peptide with or without 2 ng/mL porcine TGF-β (R&D Systems) as described previously . A blocking anti-TGF-β (clone 1D11, R&D Systems) or mouse IgG1 control (clone 11711, R&D Systems) was added at a final concentration of 20 μg/mL. After 5 days cultures were stained with CD4-PacificBlue, Vβ5-FITC, CD25-APC (BD) and Foxp3-PE (eBioscience) and analyzed by FACS.

Coculture of DC subpopulations with T cells in vitro

As indicated in the respective figure legends total $CD11c^+$ or $CD11c^-$ cells or sorted migratory $CD11c^+$ $CD40^{hi}$ or resident $CD11c^+$ $CD40^{low}$ DCs were sorted from skin-draining lymph nodes of WT or K5-mOVA mice or the indicated homozygous or heterozygous crossings with $CCR7^{-/-}$ mice. The sorted cell populations were matured with LPS (1 μg/mL, SIGMA) plus anti-CD40 (3/23, 5 μg/mL, BD) and cultured at titrated amounts with $OVA_{323-339}$-specific 5×10^4 BO97 hybridoma T cells (BO97.10.5, OVA-specific and I-Ab-restricted, was a gift from Philippa Marrack, Jewish Medical Center, Denver, CO, USA). After 24 h the culture supernatants were collected and tested for their IL-2 content by ELISA (BD). OT-I $CD8^+$ T cells and OT-II × $RAG\text{-}1^{-/-}$ $CD4^+$ T cells were purified by magnetic cell sorting (Dynal) and labeled with CFSE. In total, 30 000 DCs and T cells were mixed at a 1:1 ratio in the presence of anti-CD40 (5 μg/mL, BD) and LPS (1 μg/mL, Sigma) to achieve full DC maturation and cultured for 60 h at 37°C, 5% CO_2. As a positive control, $OVA_{257-264}$ or $OVA_{327-339}$ peptides were added to the T-cell cultures with WT migratory DCs. FACS staining included counterstainings for CD69 and CD25 (BD).

Visualization of FITC-transporting migratory DCs

FITC isomer I (Sigma) was dissolved in DMSO (Stock concentration 0.5 mg/mL) and mixed with 1:1 acetone/dibutylphtalate (Sigma) to a final FITC concentration of 0.5% w/v as described [45] and modified [64]. A volume of 100 μL of this 0.5% FITC solution was painted on the shaved abdomen of the mice. After 1, 2, 4 or 6 days, the draining axillary, brachial and inguinal lymph nodes were colleted from those mice. Cells were digested and separated as described above. For FACS analysis, cells were stained with CD11c-APC (HL-3) and CD40-biotin (3.23) followed by streptavidine-PerCP (BD) for 30 min on ice.

Immunofluorescence and confocal microscopy

To detect nuclear translocation of Rel/NF-κB transcription factors, DCs were isolated from peripheral lymph nodes of untreated or FITC-painted mice as described above and FACS-sorted according their expression of CD11c and $CD40^{low}$ or $CD40^{high}$. Cytospin preparations of the isolated DCs were dried overnight at room temperature, fixed in 4% formaldehyde and permeabilized with 0.2% Triton X-100 followed by blocking in 1:20 diluted donkey serum for 20 min. For immunofluorescence staining anti-mouse RelB Ab (Santa Cruz, rabbit polyclonal, 1:50 dilution), anti-mouse RelA Ab (Santa Cruz, rabbit polyclonal, 1:50 dilution) or anti-mouse cRel (Santa Cruz, rabbit polyclonal, 1:50 dilution) were used, followed by an anti-rabbit Cy3 Ab (1:500, Jackson Immunoresearch), each 30 min at room temperature. Slides were mounted with Fluoromount-G (Southern Biotechnology Associates) containing DAPI and images were taken with a confocal microscope (Leica TCS SP2, Wetzlar, Germany). To determine the MFI of nuclear RelB, RelA and cRel, a distinct area of the nuclei (40–47 μm^2) from 20–30 cells per condition was analyzed by Leica LCS software.

Immunohistochemistry

To detect MHC II in skin sections from the indicated bone marrow chimeras or WT control mice anti-MHC II staining was combined with hematoxylin staining. Briefly, cryostat sections (9 μm) were fixed with 4% paraformaldehyde, incubated with 10% BSA/PBS to block unspecific binding of immunoglobulins and stained with a pure rat MHC II (clone 2G9, BD) or a rat IgG2a isotype control mAb (BD) followed by an rat IgG-biotin mAb (BA-4001, Vector, U.S.), a streptavidin–AB complex (DAKO) and development with 3,3′-diaminobenzidine substrate (Fluka). Sections were counterstained with hematoxylin, dehydrated in a graded series of ethanol (76–100%) and embedded with permanent mounting medium (Eukitt, Merck).

Statistical analysis

The paired Student's *t*-test (Microsoft Excel software) was used for determining the significance of experiments. $p < 0.05$ were considered as statistically significant.

Acknowledgements: Transgenic and knockout mice or reagents were kindly provided by Horst Bluethmann, Manfred Kopf and Francis Carbone. We thank Gerold Schuler and Thomas Hünig for their generous support of this project; Khash Khazaie, Ludger

© 2011 WILEY-VCH Verlag GmbH & Co. KGaA, Weinheim

Klein and Francis Carbone for critical reading of the manuscript and helpful comments; Susanne Rößner and Melanie Schott for expert technical assistance; Katrien Pletinckx and Isabell Senft for their help on mouse preparations, Martin Väth for his help with confocal microscopy and Uwe Appelt and Christian Linden for cell sorting. This work was supported by the Deutsche Forschungsgemeinschaft (DFG) through the Interdisciplinary Center for Clinical Research Erlangen (IZKF) for N.K. and M.B.L., the Collaborative Research Center (SFB643) for H.A. and M.B.L., the Transregio Collaborative Research Centre (TR52) for A.D., M.L., F.B.S. and M.B.L. and the Graduate Program (GK520) for A.D. and M.B.L.

Conflict of interest: The authors declare no financial or commercial conflict of interest.

References

1 Reis e Sousa, C., Toll-like receptors and dendritic cells: for whom the bug tolls. *Semin. Immunol.* 2004. **16**: 27–34.

2 Steinman, R. M., Turley, S., Mellman, I. and Inaba, K., The induction of tolerance by dendritic cells that have captured apoptotic cells. *J. Exp. Med.* 2000. **191**: 411–416.

3 Probst, H. C., Lagnel, J., Kollias, G. and van den Broek, M., Inducible transgenic mice reveal resting dendritic cells as potent inducers of CD8+ T cell tolerance. *Immunity* 2003. **18**: 713–720.

4 Sixt, M., Kanazawa, N., Selg, M., Samson, T., Roos, G., Reinhardt, D. P., Pabst, R. et al., The conduit system transports soluble antigens from the afferent lymph to resident dendritic cells in the T cell area of the lymph node. *Immunity* 2005. **22**: 19–29.

5 Apostolou, I. and von Boehmer, H., In vivo instruction of suppressor commitment in naive T cells. *J. Exp. Med.* 2004. **199**: 1401–1408.

6 Abbas, A. K., Lohr, J., Knoechel, B. and Nagabhushanam, V., T cell tolerance and autoimmunity. *Autoimmun. Rev.* 2004. **3**: 471–475.

7 Salomon, B., Lenschow, D. J., Rhee, L., Ashourian, N., Singh, B., Sharpe, A. and Bluestone, J. A., B7/CD28 costimulation is essential for the homeostasis of the CD4+CD25+ immunoregulatory T cells that control autoimmune diabetes. *Immunity* 2000. **12**: 431–440.

8 Benson, M. J., Pino-Lagos, K., Rosemblatt, M. and Noelle, R. J., All-trans retinoic acid mediates enhanced T reg cell growth, differentiation, and gut homing in the face of high levels of co-stimulation. *J. Exp. Med.* 2007. **204**: 1765–1774.

9 Yamazaki, S., Dudziak, D., Heidkamp, G. F., Fiorese, C., Bonito, A. J., Inaba, K., Nussenzweig, M. C. and Steinman, R. M., CD8+ CD205+ splenic dendritic cells are specialized to induce Foxp3+ regulatory T cells. *J. Immunol.* 2008. **181**: 6923–6933.

10 Coombes, J. L., Siddiqui, K. R., Arancibia-Carcamo, C. V., Hall, J., Sun, C. M., Belkaid, Y. and Powrie, F., A functionally specialized population of mucosal CD103+ DCs induces Foxp3+ regulatory T cells via a TGF-beta and retinoic acid-dependent mechanism. *J. Exp. Med.* 2007. **204**: 1757–1764.

11 Guilliams, M., Crozat, K., Henri, S., Tamoutounour, S., Grenot, P., Devilard, E., de Bovis, B. et al., Skin-draining lymph nodes contain dermis-derived CD103(-) dendritic cells that constitutively produce retinoic acid and induce Foxp3(+) regulatory T cells. *Blood* 2010. **115**: 1958–1968.

12 Tarbell, K. V., Yamazaki, S. and Steinman, R. M., The interactions of dendritic cells with antigen-specific, regulatory T cells that suppress autoimmunity. *Semin. Immunol.* 2006. **18**: 93–102.

13 Lutz, M. B. and Schuler, G., Immature, semi-mature and fully mature dendritic cells: which signals induce tolerance or immunity? *Trends Immunol.* 2002. **23**: 445–449.

14 Ohl, L., Mohaupt, M., Czeloth, N., Hintzen, G., Kiafard, Z., Zwirner, J., Blankenstein, T. et al., CCR7 governs skin dendritic cell migration under inflammatory and steady-state conditions. *Immunity* 2004. **21**: 279–288.

15 Lutz, M. B., Döhler, A. and Azukizawa, H., Revisiting the tolerogenicity of epidermal Langerhans cells. *Immunol. Cell Biol.* 2010. **88**: 381–386.

16 Menges, M., Rossner, S., Voigtlander, C., Schindler, H., Kukutsch, N. A., Bogdan, C., Erb, K. et al., Repetitive injections of dendritic cells matured with tumor necrosis factor alpha induce antigen-specific protection of mice from autoimmunity. *J. Exp. Med.* 2002. **195**: 15–21.

17 Spörri, R. and Reis e Sousa, C., Inflammatory mediators are insufficient for full dendritic cell activation and promote expansion of CD4+ T cell populations lacking helper function. *Nat. Immunol.* 2005. **6**: 163–170.

18 Bursch, L. S., Wang, L., Igyarto, B., Kissenpfennig, A., Malissen, B., Kaplan, D. H. and Hogquist, K. A., Identification of a novel population of langerin+ dendritic cells. *J. Exp. Med.* 2007. **204**: 3147–3156.

19 Ginhoux, F., Collin, M. P., Bogunovic, M., Abel, M., Leboeuf, M., Helft, J., Ochando, J. et al., Blood-derived dermal langerin+ dendritic cells survey the skin in the steady state. *J. Exp. Med.* 2007. **204**: 3133–3146.

20 Poulin, L. F., Henri, S., de Bovis, B., Devilard, E., Kissenpfennig, A. and Malissen, B., The dermis contains langerin+ dendritic cells that develop and function independently of epidermal Langerhans cells. *J. Exp. Med.* 2007. **204**: 3119–3131.

21 Bedoui, S., Whitney, P. G., Waithman, J., Eidsmo, L., Wakim, L., Caminschi, I., Allan, R. S. et al., Cross-presentation of viral and self antigens by skin-derived CD103+ dendritic cells. *Nat. Immunol.* 2009. **10**: 488–495.

22 Henri, S., Poulin, L. F., Tamoutounour, S., Ardouin, L., Guilliams, M., de Bovis, B., Devilard, E. et al., CD207+ CD103+ dermal dendritic cells cross-present keratinocyte-derived antigens irrespective of the presence of Langerhans cells. *J. Exp. Med.* 2009. **207**: 189–206.

23 Ruedl, C., Koebel, P., Bachmann, M., Hess, M. and Karjalainen, K., Anatomical origin of dendritic cells determines their life span in peripheral lymph nodes. *J. Immunol.* 2000. **165**: 4910–4916.

24 Förster, R., Schubel, A., Breitfeld, D., Kremmer, E., Renner-Muller, I., Wolf, E. and Lipp, M., CCR7 coordinates the primary immune response by establishing functional microenvironments in secondary lymphoid organs. *Cell* 1999. **99**: 23–33.

25 Sun, C., Hall, J., Blank, R., Bouladoux, N., Oukka, M., Mora, J. and Belkaid, Y., Small intestine lamina propria dendritic cells promote de novo generation of Foxp3 T reg cells via retinoic acid. *J. Exp. Med.* 2007. **204**: 1775–1785.

26 Weih, F., Carrasco, D. and Bravo, R., Constitutive and inducible Rel/NF-kappa B activities in mouse thymus and spleen. *Oncogene* 1994. **9**: 3289–3297.

27 Weih, F. and Caamano, J., Regulation of secondary lymphoid organ development by the nuclear factor-kappaB signal transduction pathway. *Immunol. Rev.* 2003. **195**: 91–105.

28 Sha, W. C., Liou, H.-C., Tuomanen, E. I. and Baltimore, D., Targeted disruption of the p50 subunit of NF-κB leads to multifocal defects in immune responses. *Cell* 1995. **80**: 321–330.

29 Azukizawa, H., Kosaka, H., Sano, S., Heath, W. R., Takahashi, I., Gao, X. H., Sumikawa, Y. et al., Induction of T-cell-mediated skin disease specific

© 2011 WILEY-VCH Verlag GmbH & Co. KGaA, Weinheim

for antigen transgenically expressed in keratinocytes. *Eur. J. Immunol.* 2003. **33**: 1879–1888.

30 **Waithman, J., Allan, R. S., Kosaka, H., Azukizawa, H., Shortman, K., Lutz, M. B., Heath, W. R. et al.,** Skin-derived dendritic cells can mediate deletional tolerance of class I-restricted self-reactive T cells. *J. Immunol.* 2007. **179**: 4535–4541.

31 **Gandhi, R., Anderson, D. E. and Weiner, H. L.,** Cutting edge: immature human dendritic cells express latency-associated peptide and inhibit T cell activation in a TGF-beta-dependent manner. *J. Immunol.* 2007. **178**: 4017–4021.

32 **Steinman, R. M., Hawiger, D. and Nussenzweig, M. C.,** Tolerogenic dendritic cells. *Annu. Rev. Immunol.* 2003. **21**: 685–711.

33 **Sakaguchi, S., Ono, M., Setoguchi, R., Yagi, H., Hori, S., Fehervari, Z., Shimizu, J. et al.,** Foxp3+ CD25+ CD4+ natural regulatory T cells in dominant self-tolerance and autoimmune disease. *Immunol. Rev.* 2006. **212**: 8–27.

34 **Shevach, E. M., DiPaolo, R. A., Andersson, J., Zhao, D. M., Stephens, G. L. and Thornton, A. M.,** The lifestyle of naturally occurring CD4+ CD25+ Foxp3+ regulatory T cells. *Immunol. Rev.* 2006. **212**: 60–73.

35 **Steinman, R. M., Hawiger, D., Liu, K., Bonifaz, L., Bonnyay, D., Mahnke, K., Iyoda, T. et al.,** Dendritic cell function in vivo during the steady state: a role in peripheral tolerance. *Ann. N. Y. Acad. Sci.* 2003. **987**: 15–25.

36 **Oldenhove, G., de Heusch, M., Urbain-Vansanten, G., Urbain, J., Maliszewski, C., Leo, O. and Moser, M.,** CD4+ CD25+ regulatory T cells control T helper cell type 1 responses to foreign antigens induced by mature dendritic cells in vivo. *J. Exp. Med.* 2003. **198**: 259–266.

37 **Yamazaki, S., Iyoda, T., Tarbell, K., Olson, K., Velinzon, K., Inaba, K. and Steinman, R. M.,** Direct expansion of functional CD25+ CD4+ regulatory T cells by antigen-processing dendritic cells. *J. Exp. Med.* 2003. **198**: 235–247.

38 **Banerjee, D., Dhodapkar, M., Matayeva, E., Steinman, R. and Dhodapkar, K.,** Expansion of FOXP3high regulatory T cells by human dendritic cells (DCs) in vitro and after injection of cytokine-matured DCs in myeloma patients. *Blood* 2006. **108**: 2655–2661.

39 **Yamazaki, S., Bonito, A. J., Spisek, R., Dhodapkar, M., Inaba, K. and Steinman, R. M.,** Dendritic cells are specialized accessory cells along with TGF-b for the differentiation of Foxp3+ CD4+ regulatory T cells from peripheral Foxp3– precursors. *Blood* 2007. **110**: 4293–4302.

40 **Akbari, O., DeKruyff, R. H. and Umetsu, D. T.,** Pulmonary dendritic cells producing IL-10 mediate tolerance induced by respiratory exposure to antigen. *Nat. Immunol.* 2001. **2**: 725–731.

41 **Jiang, A., Bloom, O., Ono, S., Cui, W., Unternaehrer, J., Jiang, S., Whitney, J. A. et al.,** Disruption of E-cadherin-mediated adhesion induces a functionally distinct pathway of dendritic cell maturation. *Immunity* 2007. **27**: 610–624.

42 **Watanabe, N., Wang, Y. H., Lee, H. K., Ito, T., Cao, W. and Liu, Y. J.,** Hassall's corpuscles instruct dendritic cells to induce CD4+CD25+ regulatory T cells in human thymus. *Nature* 2005. **436**: 1181–1185.

43 **Salomon, B., Cohen, J. L., Masurier, C. and Klatzmann, D.,** Three populations of mouse lymph node dendritic cells with different origins and dynamics. *J. Immunol.* 1998. **160**: 708–717.

44 **Henri, S., Vremec, D., Kamath, A., Waithman, J., Williams, S., Benoist, C., Burnham, K. et al.,** The dendritic cell populations of mouse lymph nodes. *J. Immunol.* 2001. **167**: 741–748.

45 **Kissenpfennig, A., Ait-Yahia, S., Clair-Moninot, V., Stossel, H., Badell, E., Bordat, Y., Pooley, J. L. et al.,** Disruption of the langerin/CD207 gene abolishes Birbeck granules without a marked loss of Langerhans cell function. *Mol. Cell Biol.* 2005. **25**: 88–99.

46 **Carrasco, D., Ryseck, R. P. and Bravo, R.,** Expression of relB transcripts during lymphoid organ development: specific expression in dendritic antigen-presenting cells. *Development* 1993. **118**: 1221–1231.

47 **Weih, F., Carrasco, D., Durham, S. K., Barton, D. S., Rizzo, C. A., Ryseck, R. P., Lira, S. A. and Bravo, R.,** Multiorgan inflammation and hematopoietic abnormalities in mice with a targeted disruption of RelB, a member of the NF-kappa B/Rel family. *Cell* 1995. **80**: 331–340.

48 **Wu, L., D'Amico, A., Winkel, K. D., Suter, M., Lo, D. and Shortman, K.,** RelB is essential for the development of myeloid-related CD8alpha- dendritic cells but not of lymphoid-related CD8alpha+ dendritic cells. *Immunity* 1998. **9**: 839–847.

49 **Weih, F., Durham, S. K., Barton, D. S., Sha, W. C., Baltimore, D. and Bravo, R.,** Both multiorgan inflammation and myeloid hyperplasia in RelB-deficient mice are T cell dependent. *J. Immunol.* 1996. **157**: 3974–3979.

50 **Grumont, R., Hochrein, H., O'Keeffe, M., Gugasyan, R., White, C., Caminschi, I., Cook, W. and Gerondakis, S.,** c-Rel regulates interleukin 12 p70 expression in CD8(+) dendritic cells by specifically inducing p35 gene transcription. *J. Exp. Med.* 2001. **194**: 1021–1032.

51 **Wirtz, S., Becker, C., Fantini, M. C., Nieuwenhuis, E. E., Tubbe, I., Galle, P. R., Schild, H. J. et al.,** EBV-induced gene 3 transcription is induced by TLR signaling in primary dendritic cells via NF-kappa B activation. *J. Immunol.* 2005. **174**: 2814–2824.

52 **Guilliams, M., Crozat, K., Henri, S., Tamoutounour, S., Grenot, P., Devilard, E., de Bovis, B. et al.,** Skin-draining lymph nodes contain dermis-derived CD103- dendritic cells that constitutively produce retinoic acid and induce Foxp3+ regulatory T cells. *Blood* 2010. **11**: 1958–1968.

53 **Apostolou, I., Verginis, P., Kretschmer, K., Polansky, J., Huhn, J. and von Boehmer, H.,** Peripherally induced Treg: mode, stability, and role in specific tolerance. *J. Clin. Immunol.* 2008. **28**: 619–624.

54 **Wang, L., Pino-Lagos, K., de Vries, V. C., Guleria, I., Sayegh, M. H. and Noelle, R. J.,** Programmed death 1 ligand signaling regulates the generation of adaptive Foxp3+CD4+ regulatory T cells. *Proc. Natl. Acad. Sci. USA* 2008. **105**: 9331–9336.

55 **Mahnke, K., Qian, Y., Knop, J. and Enk, A. H.,** Induction of CD4+/CD25+ regulatory T cells by targeting of antigens to immature dendritic cells. *Blood* 2003. **101**: 4862–4869.

56 **Flacher, V., Tripp, C. H., Stoitzner, P., Haid, B., Ebner, S., Del Frari, B., Koch, F. et al.,** Epidermal Langerhans cells rapidly capture and present antigens from C-type lectin-targeting antibodies deposited in the dermis. *J. Invest. Dermatol.* 2010. **130**: 755–762.

57 **Tacken, P. J., de Vries, I. J., Torensma, R. and Figdor, C. G.,** Dendritic-cell immunotherapy: from ex vivo loading to in vivo targeting. *Nat. Rev. Immunol.* 2007. **7**: 790–802.

58 **Iliev, I. D., Mileti, E., Matteoli, G., Chieppa, M. and Rescigno, M.,** Intestinal epithelial cells promote colitis-protective regulatory T-cell differentiation through dendritic cell conditioning. *Mucosal Immunol.* 2009. **2**: 340–350.

59 **Chen, W., Jin, W., Hardegen, N., Lei, K. J., Li, L., Marinos, N., McGrady, G. and Wahl, S. M.,** Conversion of peripheral CD4+CD25– naive T cells to CD4+CD25+ regulatory T cells by TGF-beta induction of transcription factor Foxp3. *J. Exp. Med.* 2003. **198**: 1875–1886.

60 **Yamazaki, S. and Steinman, R. M.,** Dendritic cells as controllers of antigen-specific Foxp3+ regulatory T cells. *J. Dermatol. Sci.* 2009. **54**: 69–75.

© 2011 WILEY-VCH Verlag GmbH & Co. KGaA, Weinheim